DERIVATION OF FOREST PLOT INVENTORY PARAMETERS FROM TERRESTRIAL LIDAR DATA FOR CARBON ESTIMATION

OM PRAKASH PRASAD KALWAR
February, 2015

SUPERVISORS:
Dr. Yousif A. Hussin
Dr. Michael J.C. Weir

DERIVATION OF FOREST PLOT INVENTORY PARAMETERS FROM TERRESTRIAL LIDAR DATA FOR CARBON ESTIMATION

OM PRAKASH PRASAD KALWAR

Enschede, The Netherlands, February, 2015

Thesis submitted to the Faculty of Geo-Information Science and Earth Observation of the University of Twente in partial fulfilment of the requirements for the degree of Master of Science in Geo-information Science and Earth Observation.
Specialization: Natural Resources Management

SUPERVISORS:
Dr. Yousif A. Hussin
Dr. Michael J.C. Weir

THESIS ASSESSMENT BOARD:
Dr. Ir. C.A.J.M. de Bie (Chair)
Dr. T. Kauranne (External Examiner, LUT Science Faculty of Technology, Finland)

ABSTRACT

Terrestrial LiDAR (T-LiDAR) technology has been evolving as a precise tool for ground forest inventory. This study was conducted to explore the potentiality of T-LiDAR technology for derivation of forest inventory parameters in primary tropical rain forest and their application in precise carbon stocks estimation to facilitate REDD+ implementation. The study was conducted in Royal Belum State Park of Malaysia.

In this study, forest sample plot inventory parameters (species, position, Diameter at Breast Height (DBH), tree height, etc.) were collected from field observations. T-LiDAR data of the sample plot was acquired through multiple scanning using a Reigl VZ-400 scanner. Pre-processing and registration of multiple scans were done in RSCAN PRO software. After that all sampled trees within the inventory plots of 500 m^2 were extracted manually in RiSCAN PRO. Then DBH and tree height were measured manually in RiSCAN PRO and CloudCompare software. Automatic derivation of DBH and tree height were also computed using Computree algorithms. The inventory parameters derived from different methods were compared to analyse the relationships between them. Above Ground Biomass (AGB) stocks of the sample plots were estimated based on both the field measured and T-LiDAR derived DBH and tree height using an allometric equation. A conversion factor (0.47) was used to convert AGB stocks to above ground carbon (AGC) stocks.

Plot wise average manual and automatic detection rate of tree was 80 % and 90 % were achieved with respect to field observations. The average of plot values of R^2 and RMSE were 0.95, 2.7 cm and 0.93, 2.29 cm respectively for manual and automatic computation of DBH. Similarly, the average of plot values of R^2 and RMSE for manual measurement and automatic derivation of tree height were 0.77, 2.96 m and 0.04 and 5.35 m respectively.

The average stocks of AGB and AGC estimated from field measured DBH and tree height were 286 Mg ha^{-1} and 134 Mg ha^{-1} respectively. While, the average stocks of AGB and AGC estimated from manually measured DBH and tree height from T-LiDAR data were 278 Mg ha^{-1} and 130 Mg ha^{-1} respectively. Similarly, the R^2 values for the estimated AGB and AGC from manually measured DBH and tree height from T-LiDAR data were 0.93 and corresponding RMSE values were 42.4 Mg ha^{-1} and 19.9 Mg ha^{-1}. The RMSE% value for AGB and AGC were 14.8% , i.e., AGB and AGC can be estimated with 14.8 accuracy with respect to field measured DBH and tree height.

Thus, this study suggests that T-LiDAR technology has potential to derive forest plot inventory parameters (stem detection, BDH, and tree height) for AGB and AGC estimation in tropical forest. Comparing with field measurement, these parameters was manually measured with reasonable accuracy from T-LiDAR data. Automatic derivation of these parameters was not very successful. There is a need to develop robust algorithms for automatic derivation of forest inventory parameters.

Keywords: Terrestrial LiDAR, point cloud data, tropical rain forest, plot inventory parameters, AGB and AGC estimation, REDD+

ACKNOWLEDGEMENTS

First of all I would like to acknowledge ITC, University of Twenty for providing a great opportunity for me complete MSc Degree and Netherlands Fellowship Program for supporting with scholarship. I am grateful to my organization for encouraging me to pursue abroad study.

I am very much indebted and grateful to my first supervisor Dr. Yousif Ali Hussin for his technical and academic support from very beginning to end of this study. He supported me with encouragement, motivation, suggestions, feedback and comments to every step of this study. His coordination with University Technology Malaysia was essential to conduct this study in the tropical forest of Malaysia. My special thanks go to my second supervisor Dr. Michael J.C. Weir, who gave me valuable suggestions and feedback during proposal construction and report writing.

My deepest appreciation goes to Dr. Ir. C.A.J.M. de Bie for his constructive comments during proposal and midterm defense. His critical and constructive comments motivated me to improve quality of this research. I also want to acknowledge the technical support of Christoph Furst from Reigl Laser Management Systems, Alexandre Piboule from Office National des Forest (Computree software) and Dr. Ram Kumar Deo from University of Minnesota St. Paul.

I would like to acknowledge am express my thanks and appreciations for The University Technology Malaysia (UTM), Razak School of Engineering and Advanced Technology for their help and supports to this research work with housing, technical and instrumental support, transportation and data collection. I am in debt to all team members who join the fieldwork in Royal Belum State Park, Perak. My special appreciation goes to Dr. Kamarrul Azhari Razak for the excellent management and organization of the fieldwork. Dr. Razak from UTM, Dr. Tan from UTM Johor Bahro are highly appreciated for their generosity in every aspect of the field campaign. The thanks and appreciation are extended to all members of the Royal Belum Expedition.

I am very much indebted to my Nepalese colleagues Mohan Joshi, Bhawana Kc, Jamuna Upreti and Sujata Budhathoki including all members of Enschede Nepali Family for their great companionship during 18 month stay in Enschede. I would like to remember all classmate of NRM batch 2013-2014. Special thanks go to Tiago Monge Santos, Nya Mwe, Buoga Jared Omondi, Fremount Banda, Maina Ben, and Dennis Ojwang Jakorado for their valuable encouragement and support from beginning to end of my studies.

Finally, my endless gratitude goes to my father and mother for being my source of inspiration throughout my life, my all relatives, friends and well wishers. My special thanks go to my wife Nitu for her sacrifices and support for further studies. I really missed my sons Ayush and Awanit, who spent their valuable childhood for 18 months without my care.

Om Prakash Prasad
Enschede, The Netherlands
February, 2015

TABLE OF CONTENTS

LIST OF FIGURES

LIST OF TABLES

LIST OF APPENDICES

LIST OF ACRONYMS

3D	Three-dimensional
AGB	Above-ground biomass
AGC	Above-ground carbon
ALS	Airborne Laser Scanner
CHM	Canopy Height Model
CO_2	Carbon Dioxide
COP	Conference of the Parties
DBH	Tree diameter at 1.3 m height form base
DTM	Digital Terrain Model
FAO	Food and Agricultural Organization (of the United Nations)
GHG	Green-house Gases
GPS	Global Position System
Ha	Hectare
INS	Internal Navigation System
IPCC	Intergovernmental Panel on Climate Change
LiDAR	Light Detection and Ranging
M	Metre
Mg	Mega gram (1000000 gram)
MRV	Measurement, Reporting, and Verification manual for REDD+
PSPs	Permanent Sample Plots
R^2	Coefficient of Determination
RBSP	Royal Belum State Park
REDD	Reduce carbon emission from deforestation and forest degradation
REDD+	Reduce carbon emission from deforestation and forest degradation and enhance conservation, sustainable forest management and forest carbon stocks
RGB	Red, Green and Blue
RMSE	Root Mean Squire Error
StdDev	Standard deviation
T-LiDAR	Terrestrial LiDAR
TLS	Terrestrial Laser Scanner
UNFCCC	United Nations Framework Convention on Climate Change

1. INTRODUCTION

1.1. Background

It is known that forest ecosystems are an important carbon reservoir. Forest vegetation sequesters carbon dioxide (CO_2) from atmosphere in the process of photosynthesis and stores it in the bark, bole, leaf, and root of trees. At present, forest covers around 31 percent of the total global land cover and stores 289 gigatonne of carbon as biomass (FAO, 2010).

Deforestation and forest degradation are the major factors contributing substantially to the climate change by adding CO_2 in the atmosphere. These phenomena are responsible for about 20% of global anthropogenic green-house gases (GHG) emissions, through agricultural expansion, conversion to pasture land, infrastructure development, destructive logging, fire etc., which are the major sources of CO_2 emission after fossil fuels use, and thus are a major causes of climate change (UN-REDD, 2008). It has been estimated that around 13 million hectares of tropical forest were converted to other uses or lost through natural causes per year in the period 2000-2010 (FAO, 2010). Therefore, it is important to reduce the emission from deforestation and land use conversion, in addition to other mitigation measures.

The United Nations Framework Convention on Climate Change (UNFCCC) has considered the need to reduce carbon emissions from deforestation and forest degradation (REDD) as one of the world's main efforts to combat climate change. The Kyoto Protocol is an international agreement linked with the UNFCCC, which binds its parties to emission reduction targets. According to the "Doha Amendment to the Kyoto Protocol", the parties are committed to reduce GHG emissions by at least 18 percent compare to the level of 1990 in the eight-year period from 2013 to 2020 (UNFCCC, 2012).

There is a growing need of accurate and effective methods for estimating biomass/carbon stocks and carbon emission to meet the requirements of both Kyoto Protocol and UN-REDD programmes (Castedo *et al.*, 2012). The use of remote sensing techniques is critical for assessing fine-scale spatial variability of tropical forest biomass/carbon stock over broad spatial extents (Clark *et al.*, 2011). Most exiting methods, which include indirect and direct measurement techniques, are limited in their capability to acquire accurate and spatially explicit measurements of forest tree-dimensional structural parameters. One of the most promising remote sensing technique is from airborne LiDAR (Light Detection And Ranging) (Andersen & McGaughey, 2004).

As for the forest ecosystem, the use of LiDAR data is particularly promising because these measurements are closely related to above ground biomass (AGB) (Hoover, 2008). LiDAR provides measurements of the horizontal and vertical vegetation structure of ecosystems. LiDAR data offers the potential use of three dimensions (3D) information, alone or in combination with satellite multispectral images, to automatically and accurately predict forest characteristics, such as- tree height, single tree detection, stem diameter, basal area, stem volume, biomass, carbon stock etc. (Montaghi *et al.*, 2013). This information is critical for estimating global carbon storage and assessing ecosystem response to climate change and natural and anthropogenic disturbances (Ni-Meister *et al.*, 2010).

The AGB is indirectly derived from LiDAR measured vegetation height or accumulated LiDAR returns from vegetation. Compared with traditional methods used to assess forest structural attributes, airborne

LiDAR data are more accurate, easy to process automatically and economically attractive (Næsset, 2011). However, large uncertainties still exist in large area AGB estimates based on airborne LiDAR (Ni-Meister *et al.*, 2010). Forest AGB is actually related to several vegetation structure parameters like tree stem volume, DBH, height, wood density and branch distribution, but height is the only structural parameter which is directly measured by airborne LiDAR (Ni-Meister *et al.*, 2010).

Terrestrial Laser Scanner (T-LiDAR), combined with automatic data processing techniques, may provide an interesting tool to bridge the gap between conventional inventory techniques and airborne laser scanning data processing schemes and to facilitate the data acquisition for 3D individual tree geometry parameters in large plots (Maas *et al.*, 2008). Recent advances in T-LiDAR technology have made LiDAR data widely available to study vegetation structure characteristics and forest biomass. T-LiDAR demonstrates promises for objective and consistent forest metric assessment, but further work is still needed to refine and develop automatic feature identification and data extraction techniques (Hopkinson *et al.*, 2004). Therefore, it is important to explore the potentiality of T-LiDAR data to estimate AGB in tropical forest.

1.2. Problem statement and justification

The countries committed to the Kyoto Protocol are required by Article 3 to submit report on the net changes in carbon sinks with specific reference to afforestation and deforestation (UNFCCC, 1997). In addition, measurement of forest carbon is a vital part of REDD+ implementation because CO_2 emission reductions and removals from forest are estimated by measuring changes in the amount of forest carbon stock, and carbon credits are also calculated by using the amount of forest carbon reserve. Therefore, the monitoring must be conducted in a manner that is reliable, transparent, and as accurate as possible, as well as feasible and acceptable .

Above ground carbon (AGC) stocks per unit area can be estimated in two basic ways: the first method is to use permanent sampling plots (PSPs) and the second method involves the use of a stand carbon stocks estimation model. In the IPCC (2006) guidelines, two methods of calculating change in carbon stocks are presented: the gain-loss method and the stock change method. In the stock change method, the change in the carbon stocks is calculated by subtracting carbon stocks measured at two different time points. The REDD+ Measurement, Reporting and Verification (MRV) manual has recommended five methods: (1) permanent sample plots; (2) over-storey height model; (3) crown diameter model; (4) community age model; and (5) radar backscattering coefficient for the estimation of tropical forest carbon (USAID, 2013).

The permanent sample plot method using ground-based inventory has advantage that deforestation and forest degradation due to land-use change are easy to detect, and because it can be used regardless of forest or vegetation type, it is very flexible. Since REDD+ requires accurate and precise estimates, a large number of plots must be established, which inevitably increases the time and effort and expense of the method. In addition, the other four indirect methods also need sufficient ground inventory data for calibration and validation of the model.

Traditional ground-based survey methods are adequate for quantification of timber volume but are normally inadequate for forest canopy characteristics (Watt & Donoghue, 2005). The accuracy of ground-based inventory depends on many factors: the selection of locations to be surveyed, the number of points or plots to be surveyed, the skill level of individuals conducting the survey, type of equipments used, and data analysis methods. Apart from these, it also depends upon the forest canopy characteristics (for example, dense, sparse, open, closed or overlapping). Therefore, there is a need for the development of a new method for ground inventory that is more accurate, fast, reliable, more objective, less expensive, and operational than the conventional methods used to date.

T-LiDAR, combines with automatic data processing techniques, may provide an alternative for the permanent sample plot method for ground-based forest inventory. T-LiDAR is one of the rapidly growing interests in photogrammetry as an efficient technology for fast and reliable characterization of 3D forest canopy via point cloud data acquisition (Tansey *et al.*, 2009). T-LiDAR provides a noble solution for collecting reference data in any forest environment. The main advantages lie in its potential to improve the accuracy and efficiency of field inventories and to provide additional features for forestry applications (Liang *et al.*, 2012).

In the 17th conference of the parties (COP) in the Durban, it was agreed that all countries would participate in the development of a new universal greenhouse gas reduction protocol that would replace the Kyoto Protocol (UNFCCC, 2011). This protocol should be completed by 2015 and put into effect in 2020. For presenting REDD+ in the new framework, methods and rules for implementing REDD+ are to be developed by 2015. Therefore, there is a need for development of a new inventory methodology for the framework. This study aim to develop more accurate methods for ground inventory data measurement.

Most of the work on application of T-LiDAR has focused on conifer, temperate broadleaf and plantation forests, while less research is conducted in tropical forests that containing very diverse canopy species (Drake *et al.*, 2002). Therefore, there is an urgent need to develop suitable inventory methods using T-LiDAR for tropical forests carbon assessment and other applications. The research has the potential to contribute to the REDD+ MRV programme by developing a new forest inventory technique to collect ground based inventory data using T-LiDAR.

1.3. Research Objectives

The main aim of this study was to derive forest sample plot inventory parameters from multiple scans of terrestrial LiDAR point cloud data and to estimate above ground biomass (AGB) and AGC stocks of the sample plots of the primary tropical rain forest in Royal Belum State Park of Malaysia.

1.3.1. Specific Objectives

1. To detect trees manually and automatically from T-LiDAR point cloud data.
2. To derive plot inventory parameters (i.e. DBH and tree height) manually and automatically from the T-LiDAR point cloud data.
3. To compare the accuracy of manually and automatically derived parameters from T-LiDAR data with respect to field measurement.
4. To estimate per hectare stocks of AGB and AGC from detected trees by T-LiDAR data in sampling plots.

1.4. Research Questions

1. How accurately are trees detected from multiple-scans of T-LiDAR point cloud data.
2. Can forest inventory parameter (i.e. DHB and tree height) be derived manually and automatically from T-LiDAR point cloud data?
3. How accurately can forest inventory parameters (i.e. DBH and tree height) be derived from the T-LiDAR data by manual and automatic methods?
4. How much AGB and AGC are stored in per hectare forest of the study area ?
5. How accurately can AGB and AGC be estimated from the T-LiDAR data?

1.5. Research hypothesis

The following two hypotheses were set to test significance of T-LiDAR derived parameters and from direct field measurements. The hypotheses were tested at critical significance level, $\propto = 0.05$.

1. H_0: There is no significant difference between DBH and tree height derived from T-LiDAR data and direct field measurement
   H_a: There is significant difference between DBH and tree height derived from T-LiDAR data and direct field measurement.

2. H_0: There is no significant difference between biomass and carbon estimated from T-LiDAR and field measurement.
   H_a: There is significant difference between biomass and carbon estimated from T-LiDAR and field measurement.

2. LITERATURE REVIEW

2.1. Laser scanning or LiDAR

Laser scanning or LiDAR (Light Detection And Ranging) is one of the active remote sensing technology in which a laser sensor transmits out pulses and accurately provides tree-dimensional profile of terrain and vegetation canopy intercepting the pulses as a function of time taken by returned energy (Calders *et al.*, 2014). For terrestrial applications, LiDAR sensors generally in operate near infrared wavelengths range of 900-1064 nanometres where vegetation reflectance is high(Lefsky *et al.*, 2002). Because absorption is very low in this range compared to visible wavelengths, a large amount of energy would return to the sensor.

Airborne LiDAR device is composed of three principal components: (i) the LiDAR Sensor, (ii) the Internal Navigation System (INS), and (iii) Global Position System (GPS). The scanner emits infrared laser beams and records the difference in time between emission of laser beams and the reception of the reflected signal. A mounted mirror in front of the laser rotates and deflects the pluses at an angle and, back and forth along a line. The position and orientation of the scanner is determined by GPS. The orientation of the scanner is determined by the INS.

The laser beam from the sensor illuminates targets in an elliptical area is called footprint. The distance between the source (sensor) and target is half of the product of the speed of light and the total time of pulse transmission to reception. Measurement of the polar and azimuthal direction of the emitted laser beam, the 3D coordinates of the reflection can be allocated in sensor's own coordinate system or GPS (Gábor, 2013). In addition, spectral characteristics (intensity, amplitude and true colour) of the target object also can be recorded which characterize the reflectance properties of the target object.

There are many types of platform for LiDAR sensor, a fixed tripod, motor vehicle, aircraft or satellite. On the basis of platform, a LiDAR can be distinguished as ground based or terrestrial (TLS), mobile, airborne (ALS) and spaceborne laser scanning systems (Figure 2-1).

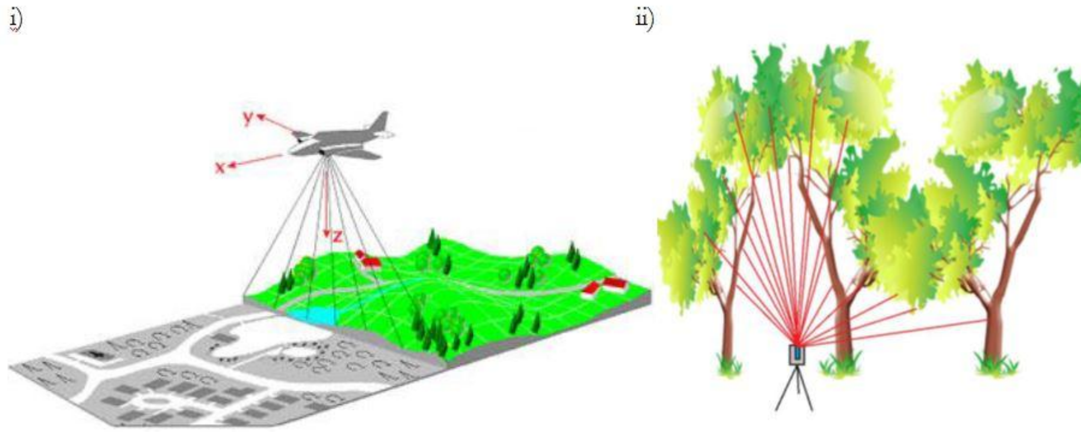

Figure 2-1. Illustration of laser scanning platforms. i) airborne and ii) terrestrial (Gábor, 2013)

2.2. T-LiDAR

T-LiDAR is an active remote sensing technology that operates from a fixed ground position. It uses laser range finding with high measuring frequency to obtain 3D coordinates and reflectance data of high spatial density and accuracy (Gábor, 2013). The operating system of a T-LiDAR is shown in Figure 2-2. It works on the principle of emission-reception of laser beam. The emitted beam is deflected by a rotating mirror and reflections from the encountered objects, result into a scene (Dassot *et al.*, 2011). Each reflected beam allows the measurement of a distance and 3D point cloud of object surface characterized by specific 3D coordinates and intensity. This 3D representation of the object is composed of millions of points which give the surfaces view or the shape of the object.

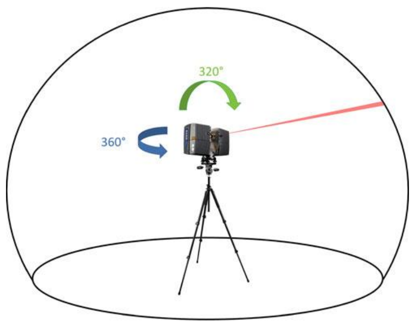

Figure 2-2. Working principle to terrestrial LiDAR (FARO)
Source: Dassot *et al.*, 2011

2.3. Types of T-LiDAR

T-LiDAR scanners can be classified into two classes according to their range measurement principle: phase-shift or pulsed time-of-flight.

2.3.1. Phase-shift scanners

In this case only one return is recorded for each direction. The distances are estimated by analyzing the phase shift between the continuously emitted and received laser beam. These scanners give wide fields of view, very high point density and fast acquisition speeds. These types of scanners are well suited for high precision and detailed measurements of relatively close target up to 100 m. They generally use visible wavelengths (600-800 nm), but scanners using infrared wavelengths are also available on the market (Dassot *et al.,* 2011).

2.3.2. Time-of-flight scanners

In this case discrete return is recorded as a point cloud. The average time of flight between emission and reception of laser pulse is calculated. These characteristics allow very long measurement but relatively low acquisition speeds. These types of scanners generally use near-infrared wavelengths (900-1500 nm) and are very suitable for 3D reconstruction of scenes at larger distances (Dassot *et al.*, 2011). These types of scanners have generally narrow vertical field of view.

Time-of-flight scanners can further be classified according to the capacity to record number of return signals computed for each direction as: (1) single return record (the first object that reflects a portion of the laser pulse; (2) first/last return record (either the first, the last or both reflected signals); (3) multiple return record (up to five signals); and (4) full waveform record (continuous signal echo) (Dassot *et al.*, 2011). For the first three technologies, only signal peaks are recorded according to specified thresholds. Both the third and fourth methods provide multi-depth information when the laser spot is not fully intercepted by the first object encountered but partially intercepted by several objects. In addition, full waveform scanners analyze the whole reflected signal, which give comparatively better assessment of the structure of the objects.

As an example, Figure 2-3 illustrates three popular terrestrial laser scanner present in the market and Table 2-1 explain their technical specifications. The plot sample data for this study was collected using Riegl VZ 400 scanner. The VZ 400 represents the new generation of pulse ranging scanner. This scanner has full-waveform digitization capacity, high measurement rate and 40% low weight compared to Riegl LMS-z 420i. The third scanner, the Leica HDS 7000 has phase comparison ranging technique, higher scanning rate but limited range. In comparison to the other two scanners, the precision is slightly better because it works on phase shift ranging method.

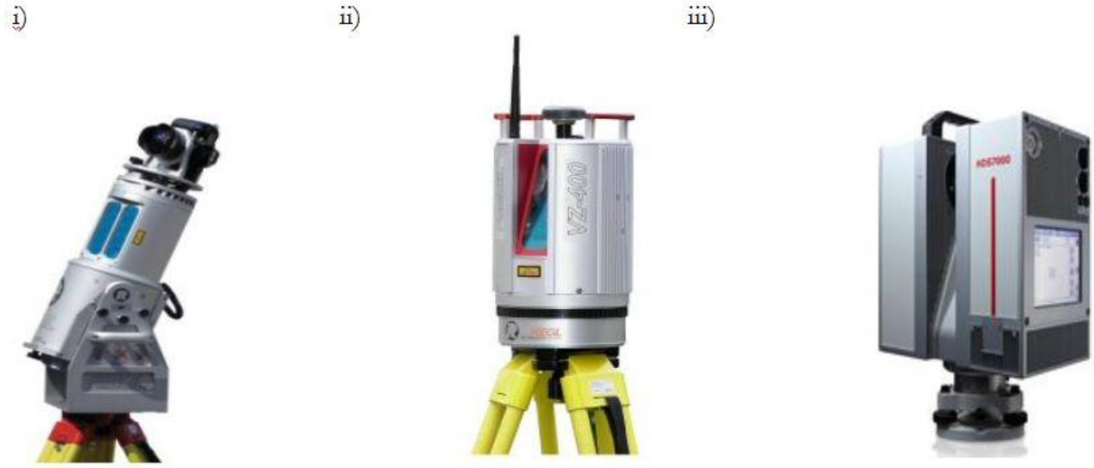

Figure 2-3. Examples on recent terrestrial laser scanners: i) Riegl LMS-Z 420i (pulse ranging) ii) Riegl VZ 400 (pulse ranging with full waveform digitization) iii) Leica HDS7000 (phase shift)

Sources: (Riegl Laser Management Systems, 2015) and (Geosystems, 2015)

Table 2-1. Comparison of technical specification of recent terrestrial laser scanners (Riegl Laser Management Systems, 2015) and (Geosystems, 2015)

Technical specification	Riegl LMS-Z 420i	Riegl VZ 400	Leica HDS 7000
Ranging method	Pulse ranging	Pulse ranging (full wave form)	Phase shift
Maximum range (m)	350-1000	280-600	187
Precision (mm)	4	3	1-9
Accuracy (mm)	10	5	5
Beam divergence (mrad)	0.25	0.35	<0.3
Footprint size at 100 m (mm)	25	30	<30
Measurement rate (kHz)	8-11	42-122	1016
Line scan angle range (degree)	80	100	320
Weight (kg)	16	9.6	9.8

From the view-point of forestry related application, technical and physical characteristic requirement of laser scanner suitable for forestry survey are: a minimum data acquisition range of 50 m, a scanning rate of 10,000 points per second for field-time efficiency, an hemispherical field of view for data acquisition flexibility, and a footprint size of 10 mm to allow for adequate measurement for stem diameter (Maas *et al.,* 2008).

2.4. Previous work

The amount of research works about the application of T-LiDAR in the tropical forest is limited because of new development of the technology in the field of forest inventory. Also, until now, few studies have been conducted in temperate coniferous, deciduous and plantation forests to derive forest inventory parameters using T-LiDAR data. The following literatures were reviewed to understand the recent development.

Hopkinson et al. (2004) conducted a research to test the potential utility of tree-level forest mensuration on plots in two forest, one in pine (*Pinus resinosa Ait.*) plantation and another in a mixed deciduous stand dominated by sugar maple (*Acer saccharum Marsh*). They found that the timber volume estimates for both plots were within 7% of manually derived estimates. Tree height and DBH parameters have the potential for objective measurement but locating and counting trees need assistance of field data with some subjective interpretation. According to them, T-LiDAR has potential for objective and consistent forest metric assessment, but there is a need to develop automatic techniques for inventory parameter extraction.

Watt et al. (2005) tested the potentiality of T-LiDAR for the extraction of tree inventory parameters in dense forest. They concluded that accurate measurements of tree diameter could be derived directly from the laser scan point cloud return in instances where the sensor's view of the tree is not obstructed. As the shadowing caused by tree density or branching frequency increased, the amount of useful information contained in the scan decreases. They calculated R^2 value of 0.92 for DBH between scanner-derived and measured value, with some form of non-linear least squares shape fitting method. They used manual measurements of the point cloud to derive stem diameter and used a maximum of two scan positions per plot.

Tansey *et al.,* (2009) used multiple scans to map a plantation of coniferous tree. They applied Hough transformation method for automatic detection of stem and measured DBH with two least-square shape-fitting algorithms. The RMSE for DBH measurement was found in the range 1.9-3.7 cm, using tree measurements. The height estimation was not successful due to upper diameter and height of tree could not be measure due to high stand density (1000 stems ha^{-1}).

Vonderach et al. (2012) applied VEVI (volume estimation by voxel intersection) algorithm based on voxel structure to estimate volume and carbon of 9 urban trees. They found the estimated volume agree with the control value within a range of -5.1% to +14.3%. Estimate of DBH correspond to the measured control values with only marginal deviations. Height estimates were systematically lower than manually measured tree heights.

Eysn et al. (2013) applied semi-automatic method for the extraction of branch and stem structure based on equirectangular projections (range and intensity map). In this method, they digitize branches and stems based on 2D maps for raster processing. The modelling is performed for each scan point individually rather than registered in a point cloud. This approach provided better handling of registration errors and wind distortions in the point cloud. The limitations for this method are reduced visibility in upper tree parts due to the scan position and area close to the zenith not being mapped.

The study sits of previous studies were in plantation or temperate coniferous/deciduous forest. These studies demonstrate that the use of T-LiDAR to derive forest inventory parameters is feasible to some extent. Efficient use of 3D T-LiDAR point data leads to next generation precision's forestry (Holopainen *et al.,* 2014). This study tests the potentiality of T-LiDAR to measure forest plot inventory parameters in tropical forest for precise estimation of forest carbon.

3. MATERIALS AND METHODS

3.1. Study area

The study area was located at the Belum State Park (RBSP), which is situated in the north of Perak State, Malaysia. It covers around 300,000 hectares of pristine rainforest known as Belum Temenggor Forest Complex and consists of several forest reserve areas, including Royal Belum State Park. This rainforest is one of the oldest rainforest, estimated to be more than 130 million year (Suksuwan, 2006). The RBSP is bordered by Thailand to the north, the state of Kelantan to the east, and Sungai Gadong to the west. The east-west highway runs along its southern boundary and has divided the forest complex separating the park area from Temenggor Forest Reserve to the south. The landscape of RBSP consists of forest, grassland, and abandoned agricultural land, and a large man-made lake called Tasik Temenggor. The park is managed by the Perak State Parks Corporation under the Perak State Parks Corporation Enactment 2001.

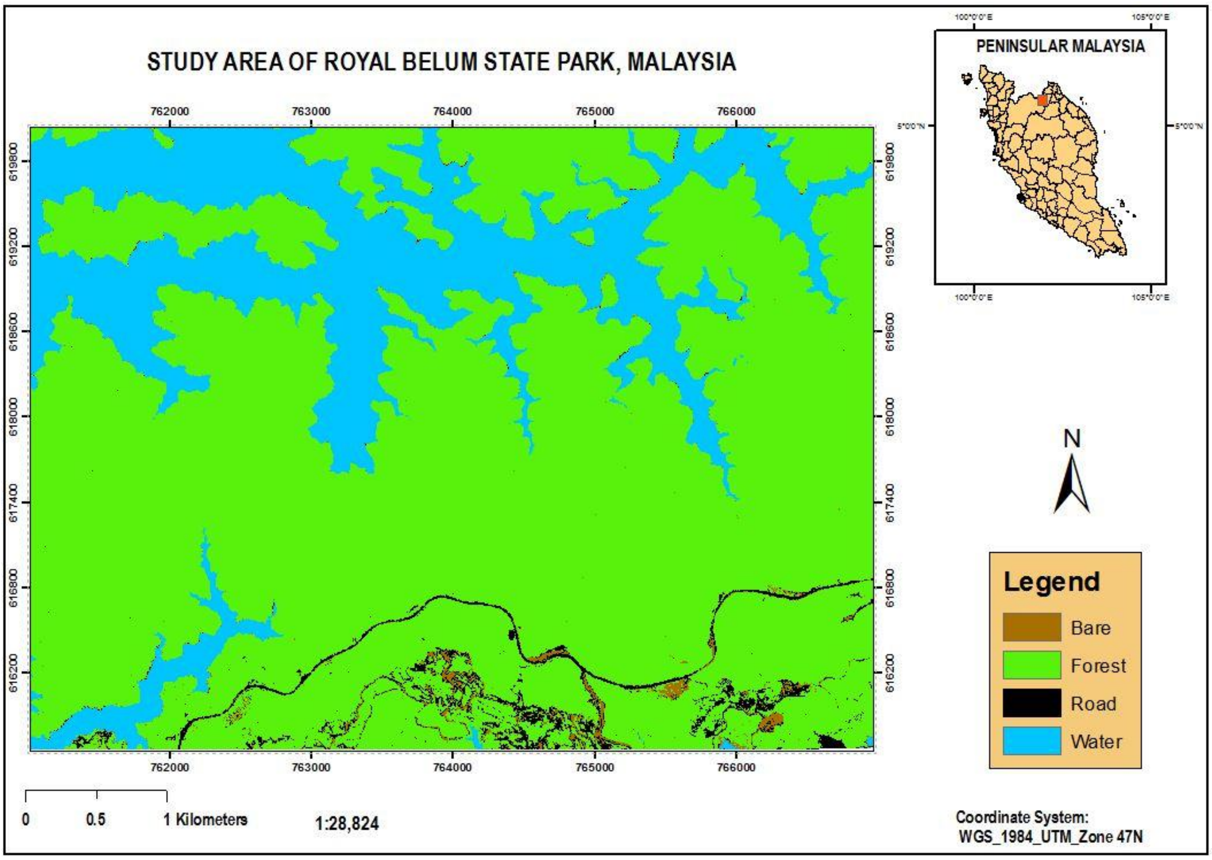

Figure 3-1. Map showing location of the study area (inset, location in Malaysia)

The location of the study area in RBSP is shown in the Figure 3-1. The major land cover types of the study area are forest, and water. The main forests types found in the area are lowland Dipterocarp, hill Dipterocarp and upper Dipterocarp forests cover from 260m to 1533m above the sea level. The majority of the forest species are characteristic of the tropical rainforest that in the Peninsular Malaysia. Hornbill, seladang, Asian elephant and Malayan tiger are important wildlife species found in the area. Orang Asli is the only human inhabitants within the RBSP. Other human settlements close to the park are Temiar and Jahai of Orang Asli ethnic group.

3.2. Materials

3.2.1. Field instruments and image used

Different sophisticated instruments were used to measure forest inventory parameters. Field instruments used for the study were RIEGL VZ-400, iPAQ, GPS, Silva Compass, Suunto Clinometer, Spherical densiometer, Range finder, Diameter tape (5m), Measuring tape (30m) and data recording sheet. The details of field instruments and their uses are given in Table 3-1.

Table 3-1. List of instruments and image used in field for data collection

Instruments	Purposes
RIEGL VZ-400	Terrestrial laser scanning
Garmin GPS	Navigation and positioning
Leica DISTO D5	Tree height measurement
Hemispherical camera	Canopy density
Silva Compass	Plot delineation and locating T-LiDAR position
Suunto Clinometer	Slop measurement
Spherical densiometer	Forest crown density measurement
Diameter tape (5m)	DBH measurement
Measuring tape (30m)	Plot delineation
Worldview-2 image	Sample plot identification

3.2.2. Software and tools

Different software packages were used for processing and analysis of point cloud. The software used in the study and their specific purpose are listed in the Table 3-2. Among them CloudCompare, Computree and RStudio are open source software.

Table 3-2. List of software and its use purposes

Software	Purposes
RiSCAN PRO	Multiple -scan registration, preprocessing, and manual measurements
ColudCompare	Slicing, cylinder fitting, manual measurements
CompuTree	Creating digital terrain model, automatic DBH measurement
ArcGIS 10.2.2	Digital elevation model analysis
Erdas Imagine 2013	Image processing
RStudio	Statistical analysis
MS Office 2010	Data analysis and thesis writing

3.3. Methods

The three major activities were carried out for conducting this research. They were field data collection, data analysis, and biomass and carbon estimation. In the field, both biometric and point cloud data were collected. In biometric data, tree species, height, DBH, crown base height, crown diameter and plot crown density were recorded from direct observations. Point cloud data was collected using RiEGL VZ-400 T-LiDAR. RiSCAN PRO software was used for pre-processing, registration of multiple-scans, and manual measurement of tree parameters. Computree software ("Computree," 2013), an open source software, was used for tree detection, and automatic measurement of DBH and tree height from registered point cloud data of sample plot. Digital terrain model (DTM) generation, horizontal slicing of trees, and cylinder fitting are major steps for automatic extraction of DBH and tree height. Above ground biomass and carbon were estimated using allometric equation from both field and T-LiDAR derived DBH and height. Comparison among plot level inventory parameters, AGB and AGC derived from field measurements and T-LiDAR data were done in RStudio. The research methodology is summarized in flow diagram (Figure 3-2) and detailed explanations are presented in the following sections.

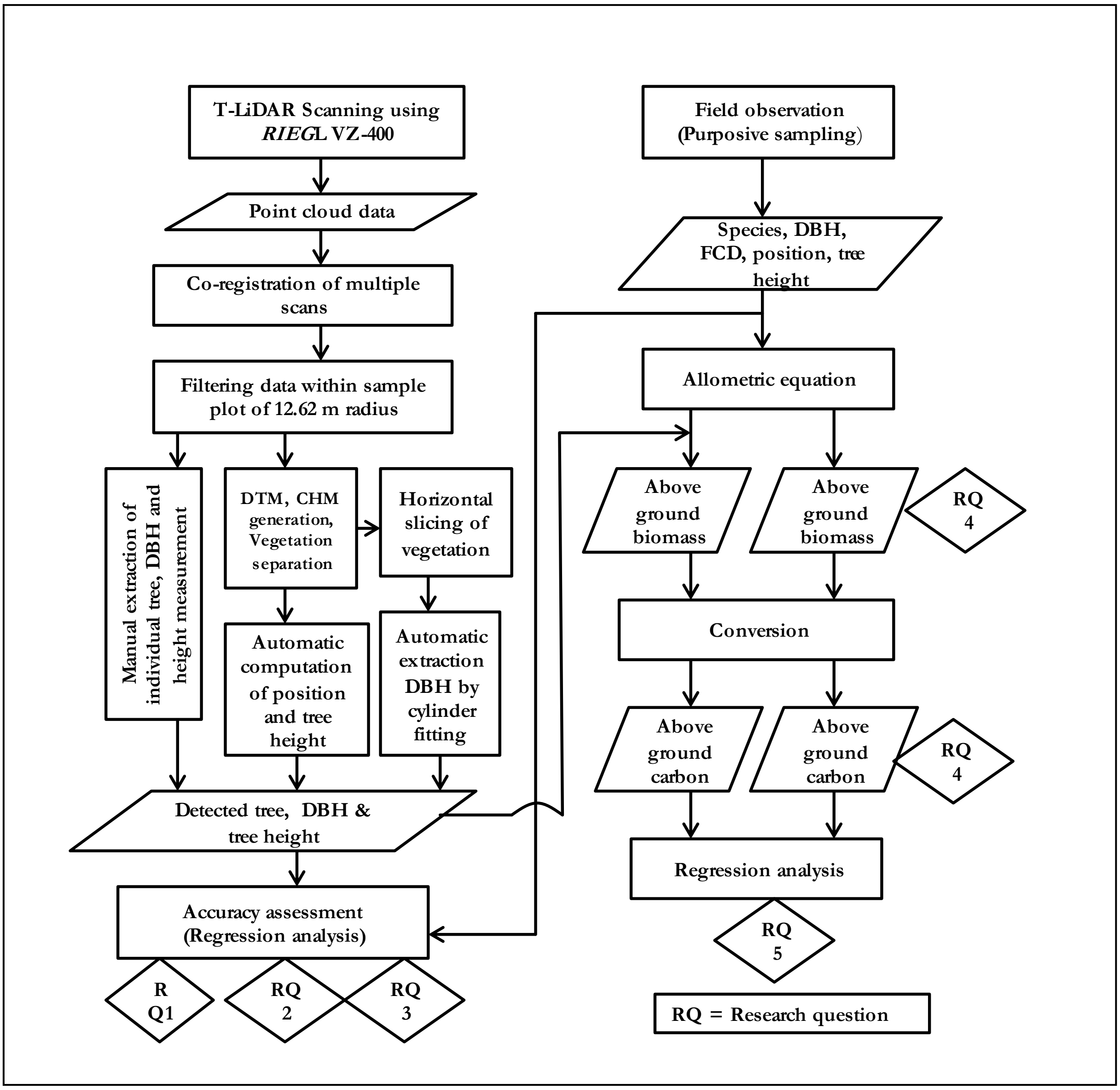

Figure 3-2. Flow diagram of research methods

3.4. Pre-fieldwork

A field schedule was prepared in advance before going to the study site. A checklist and protocols for collecting field data was prepared. The preparatory works included the followings:

- Inventory sheet for field data collection was prepared.
- Necessary field equipments were collected and condition of the equipments was checked in advance.
- Google image of the study area was down loaded and was converted into ECW format to be uploaded in Apple Inc. IPAD and made ready for navigation.
- A high resolution Worldview-2 image high resolution image of each plot was printed for the identification of tree on the image and in the field.

3.5. Determination of plot size

Determining suitable plot size is very important for collecting 3D point cloud using T-LiDAR. If a plot is large occlusion problem occurs, and if plot is small representative data cannot be acquired. Although larger plot sizes do not significantly increase the accuracy of the models, but they do increase the cost of the fieldwork. Within 15 m distance from the scanner about 95% of the trees can be successfully recognized (Trochta *et al.*, 2013). According to Ruiz et al. (2014), maximum plot size suitable for forest structure attribute estimates from LiDAR point clouds should be 500-600 m2. Therefore, for this study circular plot area of 500 m^2 with radius 12.62 m were used in flat ground. A slope correction table was used to determine the increase in the plot radius to correct for the effect of the slope of the plot.

3.6. Sampling design

Preliminary field visit was done to understand topographic condition, forest condition and accessibility into the forest. Since topography was difficult due to hilly region and T-LiDAR was also heavy (about 22 kg including camera and carrying box) to carry in the sampling land, purposive sampling strategy based on crown cover density was followed to collect plot inventory data.

Thirteen spots were determined according to the crown cover density. At each spot 2-4 circular sample plots of 500 m^2 were established at distance of at least 50m apart depending upon the size and topography of forest. Centre of the plots were chosen randomly. In few cases, centre point was shifted to choose clear field of view for T-LiDAR scan.

3.7. Plot delineation

3.7.1. Locating central position

After identification of plot, central scan positions were located such that there was minimum occlusion in the scanning . The plot centre was selected with the purpose of reducing the occlusion due to trees stems and undergrowth. The trees very close to the plot centre, cause large area behind it to be in its shadow (Liang *et al.,* 2012). The central positions were marked on the basis of ocular judgment. Since most of the plots were on sloping terrain, the central position was located such way that there was suitable and enough space for placing three outer scan positions. Positioning of tripod for TLS station is difficult on very steep slopes.

3.7.2. Plot cleaning

Some undergrowth in line of reflectors was cleared to get clear view from all four scan positions. Clearing also minimizes occlusion and gives a good scan of the bole of tree.

3.7.3. Tree tagging

Trees more than 10 cm DBH were marked with number tag. For marking the trees, A4 size plastic coated white papers marked with bold black numbers were used. All the trees within the 12.62 m radius or more in the case of sloping ground were marked with numbers (Figure 3-3).

3.8. T-LiDAR data acquisition

Each forest sample plot was scanned with Riegl VZ-400 terrestrial laser scanner. Multiple-scan, one in centre and three outside the plot (Figure 3-4), were carried out to avoid possible occlusion from surrounding vegetation. In comparison to single scan mode, the multiple scan mode give much more details of the scene but it takes more time for data acquisition and processing (Bienert *et al.,* 2006). The scanning resolution of approximately 1 cm at a distance of 10 m was selected, because this is enough to distinguish small vegetation features like small branches and leaves (Feliciano *et al.,* 2014). The following steps were followed to scan the sample plot.

3.8.1. Fixing scan positions

At first central scan position was determined and from that point outer three scan positions were marked. Tripod was placed on each scan position and the centre point was marked on the ground and GPS reading of the scan position was taken. A balanced distribution of the 3 out scan points was implemented in such a way that the angles between the out scans were around 180 degree with a circle (Figure 3-4).

3.8.2. Placing reflectors

Twelve cylindrical and four circular reflectors were placed in each plot. All the plots were full of undergrowth, and therefore sticks were used to place cylindrical reflectors. Between each central and outer scan position four cylindrical reflectors were placed in such a way that they were visible from both position. The main purpose of using of cylindrical reflectors is to register the outer scan position to the centre scan position. Circular reflectors were placed randomly on marked tree stem facing towards centre scan position. As shown in Figure 3-3, cylindrical reflectors were placed on sticks and a circular reflector was placed on tree 20. The circular reflector is used for georeferencing of the plot.

Figure 3-3. A sample plot picture of arrangement of reflectors and tree tagging

3.8.3. Setting T-LiDAR

After placing T-LiDAR on the tripod, camera was mounted on the top. Then level of the T-LiDAR was checked and legs of tripod were adjusted to minimize the roll and pitch of the TLS and instrument was set according to the technical specification given in Table 3-3.

Table 3-3. Riegl VZ-400 scanner settings for data acquisition

Beam divergence	0.35 mrad
Minimum range	1.5 m
Pulse repetition rate	300 kHz
Azimuth range	0°-360° (0.06° angular sampling)
Zenith range	30°-130° (0.06° angular sampling)
Acquisition time	About 6 minutes

3.8.4. Fixing scan position

New project was set for each plot. Within the plot, each scan was saved as new scan-position. After that instrument was set for pulse ranging scan.

3.8.5. Fine scanning of reflectors

Fine scanning of reflectors is necessary for automatic registration of multiple-scans. For fine scanning, first automatic searching of reflectors were done. After that reflectors were identified and marked manually. Then fine scanning of marked reflectors were done automatically by setting the scanner in fine scanning mode.

3.8.6. Single and multiple scan mode

A scene can be scanned in two different modes using T-LiDAR: (1) single scan; and (2) multiple scans (Figure 3-4). In the single scan method, the laser scanner is placed at a single location and only one scan is made. This method is fast, but only one side of the objects is represented in the point cloud. In the multiple scan method, generally three or four scans are taken around the objects. Then the point clouds from different scans are merged into a single point cloud. At least three reference target points are placed which can be scanned in both scans. This method ensures the complete 3D point cloud of the targets. However, it increases the field observation times and processing, which depend on the number of targets and the methods, employed, i.e. automatic or manual detection used to detect the targets. For this study multiple scans were done.

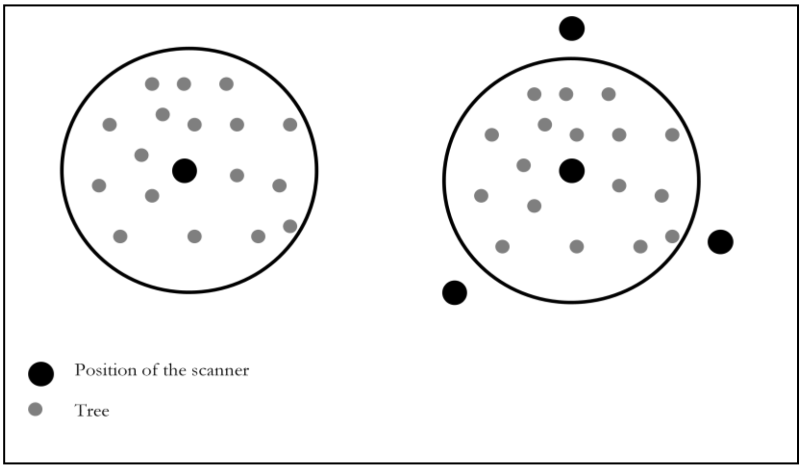

Figure 3-4. Single scan mode (left) and multiple scan mode (right) (Bienert *et al.,* 2006)

3.9. Biometric data collection

Biometric data of 35 sample plots were collected in the field inventory. The core variables measured in the field included tree height, DBH, crown diameter, and distance and azimuth of tree stems from the plot centre. According to Brown, (2002), trees below 10 cm DBH contribute little to the total biomass of forest. So only trees with 10 cm or more DBH were measured. A diameter measuring tape was used to measure DBH of trees in millimetre accuracy. In addition, other important observations i.e. aspect, slope, and exposure were recorded.

3.9.1. Tree species

Local name of each marked tree were identified with the help of a local ranger working in the area. Pictures and samples of bark of unidentified trees were taken during the forest inventory. After returning from the field, pictures and bark samples were matched with the published report to identify the tree species.

3.9.2. DBH measurement

DBH of each marked tree within a plot was measured with diameter tape at 1.3 m height above the ground. In the case of buttresses at 1.3 m, DBH was measured just at the point where buttresses end. In the case of forked trees, if the fork was below the DBH, both trunks were measured as individual tree. The DBH reading was recorded up to millimetre accuracy so that it can be compared with T-LiDAR derived DBH.

3.9.3. Height

Laser range finder (Leica DISTO D5) was used to measured height of tree. The reading of height was recorded up to centimetre accuracy. Our team faced difficulty in locating top of the tall trees due overlapping and dense crown in many sample plots.

3.9.4. Crown diameter

The crown diameter of some sample trees were measured using measuring tape. Two perpendicular measurements of projected crown over ground were made for each tree and average was recorded as a crown diameter. In each plot, 5-7 trees were measured as a reference trees.

3.10. Pre-processing of T-LiDAR Data

3.10.1. Pre-processing and multiple scans registration

RiSCAN PRO v1.8.1 software was used for pre-processing of scanned point cloud data. The scanned file was imported as a new project using 'Download and Convert' wizard of help menu. The first step in the pre-processing is the registration of the 3 outer scan positions to the central scan position. All the three outer scan positions were registered to the central scan position using tie-points. The common tie-points between two scan positions were automatically identified by the program and were registered. An example of registered plot is shown in Figure 3-5. The scans from four positions have been displayed in fuchsia, yellow, aqua, and lime colour. The black colour is shadow area due to occlusion. To minimize the error in registration of multiple-scan, 'Multi-Station Adjustment' was done. The error of multiple registration of plot varies from 11mm to 35 mm with an average of 16 mm for the 24 plots used. The standard deviation (error) in multiple scan registration of plot is given in Table 3-4.

Table 3-4. Error (standard deviation) in multiple scan registration

Plot	7	8	9	10	11	12	13	14	15	16	17	18
Error [meter]	0.018	0.018	0.035	0.013	0.011	0.015	0.015	0.016	0.020	0.015	0.020	0.022
Plot	19	21	22	23	24	25	26	27	28	30	31	32
Error [meter]	0.016	0.017	0.014	0.012	0.013	0.014	0.011	0.017	0.015	0.014	0.015	0.015

Figure 3-5. Registered scan data from four different positions is shown with different colour

3.10.2. Plot extraction

After registration of multiple scans, the next step involved filtering of the point cloud. For this all points inside the area of interest was extracted. A cylinder of radius 12.62 m (sample plot radius) was used to filter out all points outside the plot using the Computree software. Selection tool was used to extract point cloud data of the sample plots in RiSCAN PRO. The filtered point cloud was used for further processing in both manual and automatic forest inventory parameters extraction procedures. An example of registered point cloud data is shown in intensity values and the extracted sample plot is shown in RGB colour (Figure 3-6).

a) b)

Figure 3-6. a) Point cloud of registered multiple scans is displayed in intensity values; b) an extracted sample plot is displayed in RGB colour

3.11. Manual extraction of inventory parameters

3.11.1. Manual extraction of individual tree

The registered sample plot point cloud data were processed in RiSCAN PRO software for manual extraction of individual tree. Tree tag numbers were used to identify the individual tree. All point cloud representing the individual tree were separated from sample plot data using selection tool. The selection of all point cloud data associated with a single tree was performed by locating each marked individual tree stem within the entire plot point cloud and then selecting the vertical area corresponding to maximum crown diameter and tree height. In most cases the selected point cloud often included portions of canopy from surrounding trees. The individual tree point cloud data of all sample trees were visually inspected, and outlying point cloud were deleted. The manual extraction of individual trees is a time consuming task. Examples of extracted individual trees are shown in Figure 3-7.

Plot 13, Tree no. -2 Plot 24, Tree no. -12

Figure 3-7. Examples of manually extracted trees from point cloud data

3.11.2. Manual measurement of DBH from T-LiDAR data

The Diameter at Breast Height (DBH) is defined as the diameter of the stem at 1.3 m above plane ground at base of a trunk (Figure 3-8). The DBH was determined by measuring thickness of trunk at 1.3 m above the ground. It was measured using distance measuring tool in RiSCAN PRO software.

Figure 3-8. Ground point of tree on sloping terrain (left) and circle in data points representing DBH
Source: Maas *et al.,* 2008

3.11.3. Manual measurement of tree height

The tree height was measured as the difference between the lowest point (base of the trunk) and the highest point of tree. The individual tree was exported into the CloudCompare and the height was determined by fitting box in each tree as shown in the Figure 3-9.

Figure 3-9. Tree height measurement by box fitting in CloudCompare software

3.12. Automatic extraction of inventory parameters

3.12.1. Automatic extraction of DBH

Registered multiple point cloud data from RiSCAN PRO software was imported as LAS file into Computree software. Sample plot of 12.62 m radius was extracted using plug-in which was used to generate Digital Terrain Model (DTM) and to separate vegetation point cloud. The point cloud of vegetation from this step was further processed for horizontal slicing and clustering. After that, horizontal and vertical merging of logs were done to reduce the effect of occlusion. Then the cylinder was fitted and filtered to reduce the small trees of less than 10 cm diameter. After that diameter was computed by fitting circle at 1 m and 1.6 m above DTM and DBH was estimated by interpolating the reference height value at 1.3 meters. The details of steps for automatic extraction of DBH is given in Figure 3-10 (Othmani *et al.*, 2011).

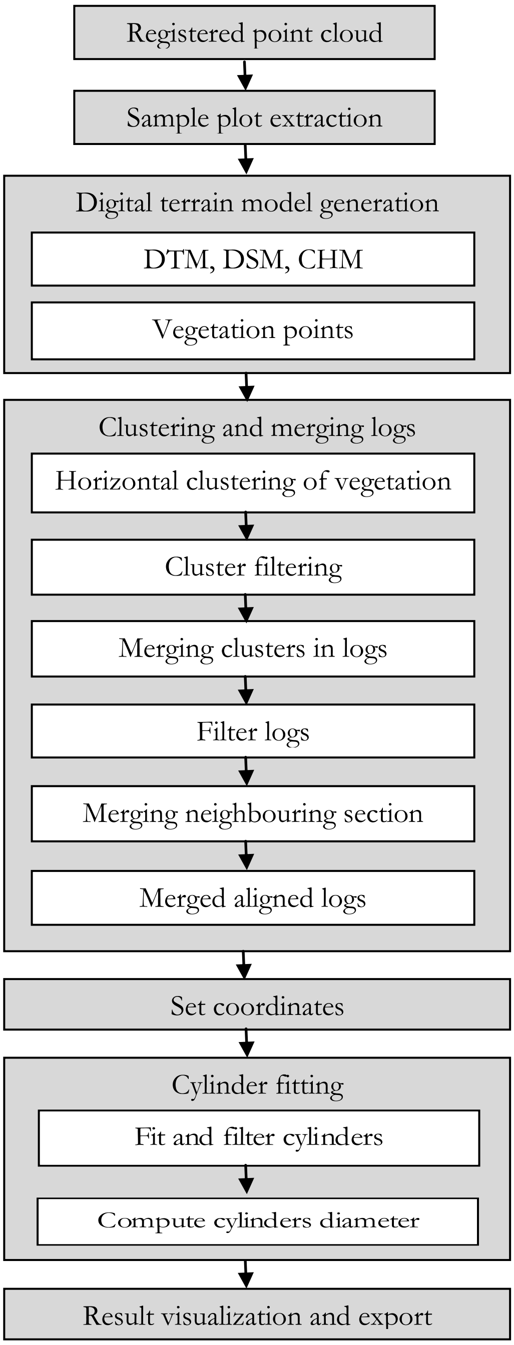

Figure 3-10. Steps for automatic extraction of DBH using Computree algorithms

3.12.2. DTM generation

Determination of tree height and DBH require the determination of a local digital terrain model. The filtered point cloud data from pre-processing was used for generating the DTM and Canopy Height Model (CHM) (Figure 3-11). A simple height histogram analysis searching for maxima in predefined XY-meshes of the laser scanner data, followed by a neighbourhood consistency check and bilinear interpolation in the meshes, provide a suitable terrain model for height reduction (Bienert *et al.,* 2006).

The DTM was generated using Computree algorithms (Othmani *et al.,* 2011). In this steps soil and vegetation points were separated. A Z grid is created at specified grid resolution (for this study, 50 cm X 50 cm was used) and for each cell, the Z value of points is stored in the "Zmin grid". The density of points between Zmin and (Zmin+32 cm) of each cell was computed. Each cell with value minimum than pre-specified point density (200 pts/m²) was classified as cell having no soil points. Then each cell is compared with the 4X4 neighbourhood cells. Each cell with no Zmin grid value is estimated as the inverse distance weighted mean of its neighbours in the triangulation.

The DTM is computed from the computed using Zmin gird values. Delaunay triangulation is used for interpolation. The points between Zmin and (Zmin+32 cm) were classified as soil points and were separated from vegetation points.

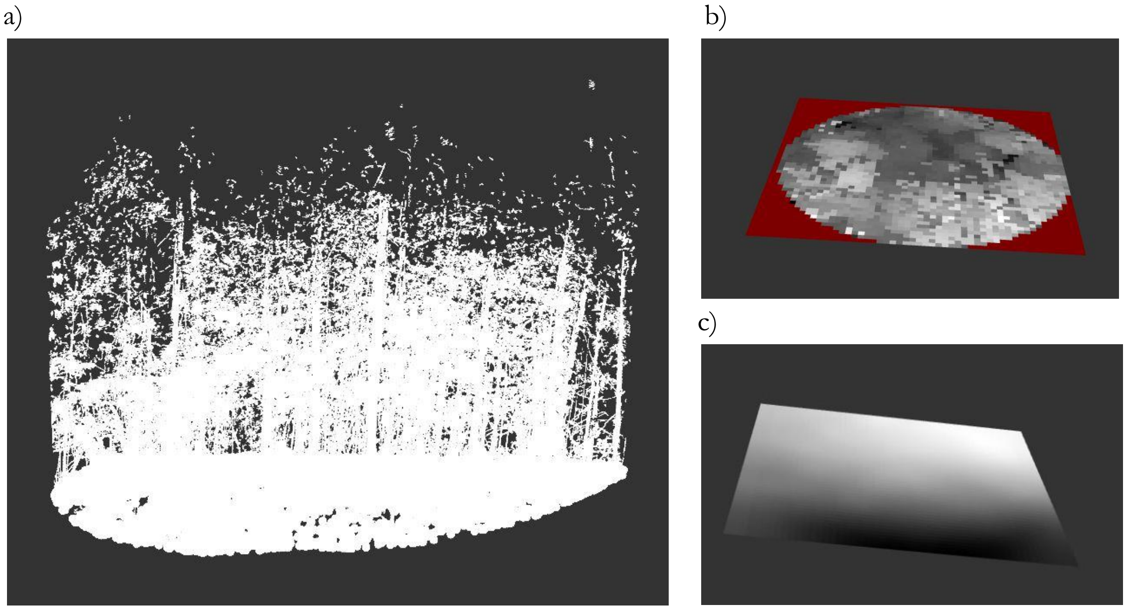

Figure 3-11. Examples: a) Extracted plot; b) CHM; and c) DTM

3.12.3. Horizontal clustering vegetation

In this step the cloud of vegetation point was sliced in Z-direction at 1 cm thick. Then points which are within 3 cm distances are grouped according to their proximity. Clusters having less than 3 points are filtered out. After that in each cluster a circle is fitted by a least square routine. The fitted circles having higher error are filtered out. Each fitted circle is analysed with respect to the fitted circles of ten Z layers below and ten Z-layers above in clusters. Circles with centres horizontally included in the observed circle, and have similar radius, were filtered for further analysis.

3.12.4. Merging clusters into logs

The goal of this step is to obtain single virtual section of tree. In this stage 1 cm thick clusters are merged to get vertically oriented virtual sections. Horizontally intersected bounding rectangles within the 50 cm Z-distance are merged into same virtual section. The bounding rectangle of a cluster is defined as the smaller XY oriented rectangle that includes all the points of the cluster(Othmani *et al.*, (2011). The log sections less than 20 clusters were filtered out. This step minimised the effect of occlusions by creating virtual sections. The end product of this step was a real tree represented by virtual sections.

3.12.5. Merging neighbouring and aligned sections

In this step virtual sections from the previous step were merged into the single tree. The virtual section was merged into skeleton slices which created a skeleton that having thickness of 10 cm. Two sections that having mutually overlapping sections and within a horizontal distance of 50 cm were merged. After that the whole skeleton formed by merging sections together was computed again and smoothed. The end product of this step was one virtual log for each original tree stem or branch.

3.12.6. Circle fitting and DBH computing

Diameter was computed by fitting circle at 1 m and 1.6 m above Digital Terrain Model (DTM) and DBH was estimated by interpolating the reference height value at 1.3 meters from the DTM (Figure 3-12 a). The position of tree was computed from the centre of the circle. The diameter of the circle gives an estimation of the DBH. The automatically computed DBH was matched with field measured DBH on the basis of size.

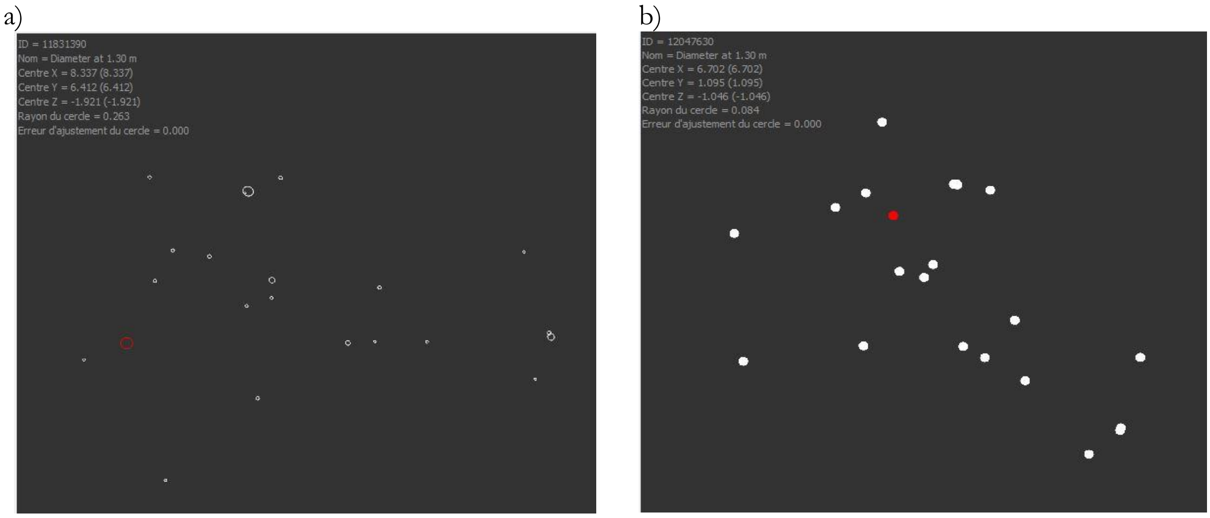

Figure 3-12. a) DBH computed by circle fitting at 1.3 m; b) Position of tree computed from centre of circle at 1.3 m (plot 30)

3.12.7. Determination of location and tree height

To locate the tree stem location, slice of tree stem layer was done in Computree software, and the tree stem centre coordinate at 1.3 m was computed as the centre of the cylinder point of T-LiDAR points defining the tree stem (Figure 3-12 b). DTM was used to set corresponding coordinate of the tree.

The tree height was computed from the CHM as the difference between the highest point of the point cloud of a tree and the representative ground point in ArcMap 10.2.2, similar procedure described by (Maas *et al.,* 2008). According to them, due to consequence of occlusions and the under sampling character of T-LiDAR, the highest point of the point cloud may not be representative of the tree height.

3.13. Above-ground Biomass and Carbon estimation

Allometric equations were used for AGB estimation from forest inventory parameters like DBH, height, and crown diameter. Choosing a suitable allometric equation is very essential for correct estimation of biomass and carbon. Since there is no species wise allometric equation suitable for the study, the general allometric equation developed by Chave *et al.,* (2005) for tropical moist forest was used for the estimation of biomass from DBH, height and density of sample tree. The allometric equation is given as below;

$$ABG = 0.0509 \times \rho D^2 H \qquad \text{..1}$$

Where,

AGB = Above-ground biomass in kg
ρ = density of wood in gm per cm^3
D = Diameter of tree at breast height in cm
H = Height three in m

This allometric equation was selected because this model has been tested for the region of Kalimantan, Balikpapan, Indonesia from 0°40' S - 116° 45' E and Kalimantan, Sebulu, Indonesia from 1°50' - 116° 58' where average rainfall is 1862 mm to 2200 mm. The climatic conditions of the Royal Belum study area are similar to those found the Kalimantan.

The global wood density data base from Dryad Digital Repository was used as a source for wood density value. The list of species specific density used for the estimation of biomass is given in Appendix 1 (Zanne et al., 2015). An average value was used for the tree species which specific density was not found in literature. After estimation of AGB, AGC was estimated using conversion factor 0.47 (IPCC, 2006).

$$Above\ Ground\ Carbon\ stock = 0.47 \times AGB \qquad \text{.......... 2}$$

3.14. Statistical analysis

Descriptive statistics (minimum, maximum, mean, standard deviation) was used to draw plot level information of both field and T-LiDAR measured inventory parameters. Regression analysis was carried out to quantify relationship between parameters and scattered plots were made to show the relationship. Coefficient of determinant (R^2) and root mean square error (RMSE) were calculated on the plot basis to compare T-LiDAR derived plot inventory parameters with field measurements. R^2 indicates how well a model can explain the reality. RMSE was calculated as follows;

$$RMSE = \sqrt{\frac{1}{n}\sum_{i=1}^{n}(X_{Oi} - X_{Pi})^2} \qquad \text{.......... 3}$$

$$RMSE\% = 100 \times \frac{RMSE}{\bar{y}} \qquad \text{.......... 4}$$

Where,

$RMSE$ = Root mean square error
X_O = Observed parameter
X_P = Predicted parameter
n = Number of observations
$\bar{y}$ = Mean of the variable in the field

Similarly, a Paired T-test was done to test the significance of T-LiDAR derived inventory parameters by using following formula;

$$t = \frac{\bar{d}}{\sqrt{\frac{s^2}{n}}} \qquad \text{.......... 5}$$

Where, t = Paired sample t test with n-1 degrees of freedom
$\bar{d}$ = Mean difference between two samples
s^2 = Sample variance
n = Sample size

4. RESULTS

4.1. Descriptive analysis of field data

The forest of Royel Belum State Park is protected primary forest and is composed of Dipterocarpaceae family. *Shorea*, *Hopea*, *Dipterocarpus* and *Vatica* are the largest genera found in the study area. Biometric data was collected from 35 sample plots of forest are 1.57 ha, from which 59 tree species were recorded. Around 62% forest area is covered by seven major species; 15% by *Syzygium,* 13% *by Vatica,* 9% by *Mastixia trichotoma Blume,* 7% by *syn. Acacia greggii,* 7% *Pimelodendrom,* 7% *by Koompassia Malaccensis* and 6% *Trypanosoma*. The list of local and scientific name the species found in the area is given in Appendix 1. The details of forest species composition are shown in Figure 4-1.

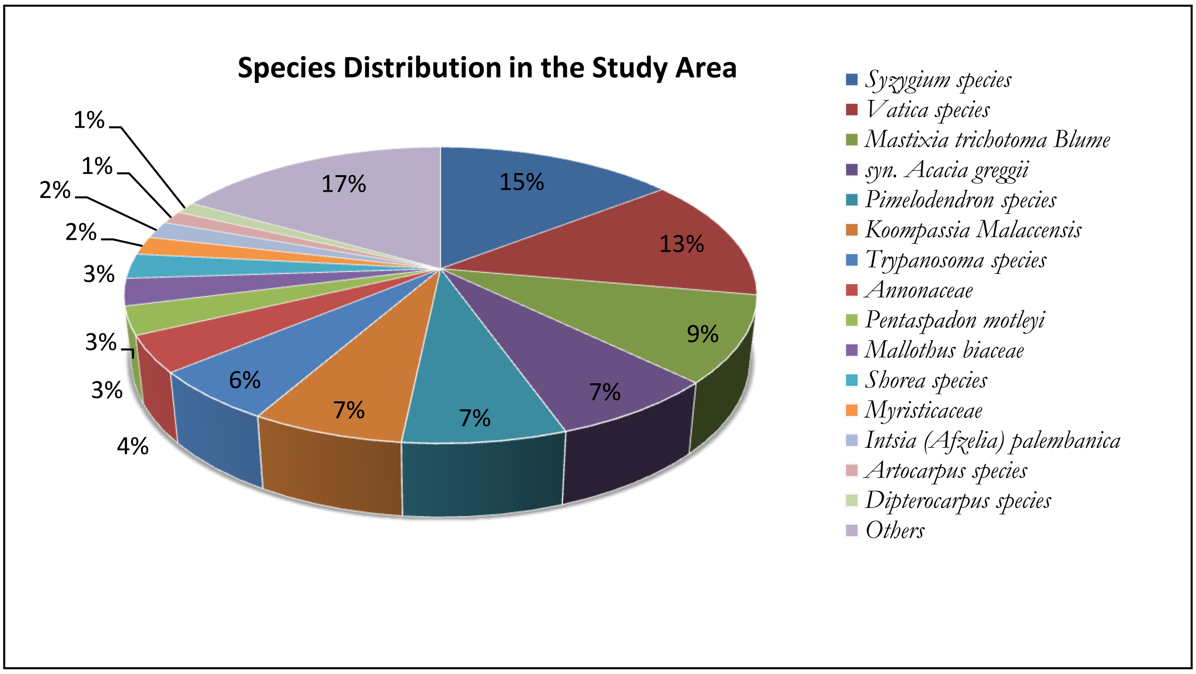

Figure 4-1. Species distribution in the study area

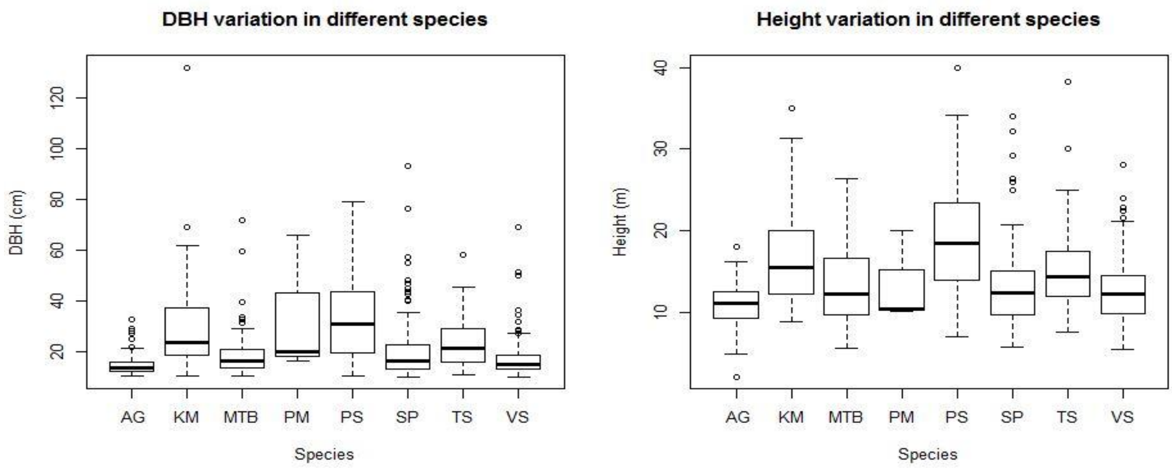

Figure 4-2. Box plot of DBH and tree height of major tree species

(AG = *syn. Acacia greggii*, KM = *Koompassia Malaccensis*, MTB = *Mastixia trichotoma Blume*, PS = *Pimelodendrom species*, SP = *Syzygium species*, TS = *Trypanosoma species*, VS = *Vatica species*)

DBH and tree height distribution of the major species were analysed and presented by means of box plots (Figure 4-2). *Pimelodendrom species* has the largest mean DBH and mean height followed by *Koompassia Malaccensis, Trypanosoma species, Syzygium species, Mastixia trichotoma Blume, Vatica species and Trypanosoma species*. This shows that a tree that has a large DBH is higher than tree having small DBH i.e., tree height depends upon the diameter.

4.2. Individual tree detection from T-LiDAR data

4.2.1. Manual extraction of individual tree

T-LiDAR data from 24 plots were analysed. Out of 35 plots, plots 1-6 were located in secondary forest, plots 20 and 29 had error in reflector scanning, and plots 33-35 were not processed due time constraint. Therefore, these plots were not included in analysis. After registration of multiple scan, point cloud data within the plot was extracted. Then point cloud of individual tree was extracted one by one using RiSCAN PRO software. A tree tag was used to recognise the individual tree. The details of the individual tree extracted from the sample plots are presented in Table 4-1. The tree extraction percentage varies from 69 to 100. All trees of plots 8, 13, 18, 15, and 21 were recognised and extracted. The main causes of lower tree reorganization in other plots were occlusion (Figure 5-8) due to high stem density and the presence of undergrowth.

Table 4-1. Details of manually detected individual tree from T-LiDAR data

Plot	*7*	*8*	*9*	*10*	*11*	*12*	*13*	*14*	*15*	*16*	*17*	*18*
Total tree	26	22	11	24	29	29	28	33	18	26	29	13
Detected tree	18	22	9	20	23	23	28	31	18	25	24	13
Extraction %	69	100	82	83	79	79	100	94	100	96	83	100
Plot	*19*	*21*	*22*	*23*	*24*	*25*	*26*	*27*	*28*	*30*	*31*	*32*
Total tree	28	25	26	30	16	26	32	24	22	22	35	23
Detected tree	25	25	25	26	15	21	24	17	19	21	33	22
Extraction %	89	100	96	87	94	81	75	71	86	95	94	96

4.2.2. Automatic detection of individual tree

The point cloud data of 24 plots have been processed in Computree software. The details of the individual tree detection from the sample plots are presented in Table 4-2. The trees detection percentage varies from 72 to 100. All trees of plots 8, and 15 were detected. The main causes of lower tree reorganization in the these plots are occlusion due to high stem density and undergrowth.

Table 4-2. Details of automatically detected individual tree from T-LiDAR data

Plot	*7*	*8*	*9*	*10*	*11*	*12*	*13*	*14*	*15*	*16*	*17*	*18*
Total tree	26	22	11	24	29	29	28	33	18	26	29	13
Detected tree	24	22	8	22	27	23	26	29	18	25	25	11
Extraction %	92	100	73	92	93	79	93	88	100	96	86	85
Plot	*19*	*21*	*22*	*23*	*24*	*25*	*26*	*27*	*28*	*30*	*31*	*32*
Total tree	28	25	26	30	16	26	32	24	22	22	35	23
Detected tree	25	22	25	27	15	23	31	20	18	20	34	19
Extraction %	89	88	96	90	94	88	97	83	82	91	97	83

4.3. DBH measurements

The diameters of trees were measured by three methods: those were (1) manual measurement in field; (2) manual measurement from T-LDAR data; and (3) automatic extraction from T-LiDAR using algorithm in Computree software. Plot level statistics (minimum, maximum, mean and standard deviation) of tree diameter measurements by the tree different methods are given in Table 4-3.

Form the table, we can see that there are similarities in plot level DBH measurement statistics (minimum, maximum, mean and standard deviation) between field measurements and manual measurements from T-LiDAR data. There is no distinct differences between these two observations, which indicates that DBH can be measured from the T-LiDAR point cloud with a reasonable accuracy.

But in the case of automatic measurement, the maximum values of plots are lower than the field measurements. Similarly, mean and standard deviation values are also lower. The main reason for low values is that some big diameter trees have not been detected in the plots by the software.

Table 4-3. Plot level statistics of DBH measured in field and DBH derived from T-LiDAR data

Plot	Field DBH (cm)				T-LiDAR DBH (cm)							
	Field measurement				Manual measurement				Automatic measurement			
	Min	**Max**	**Mean**	**Std**	**Min**	**Max**	**Mean**	**Std**	**Min**	**Max**	**Mean**	**Std**
7	10	49	18.9	9.8	10.1	48.8	18.3	10.41	11.6	34.0	15.9	5.4
8	11.1	58	22.8	10.6	10.6	52.2	21.8	9.76	12.8	41.6	21.0	7.7
9	12.4	52.5	27.5	16.0	10.1	46.5	24.5	14.77	10.6	45.4	18.2	12.9
10	11.1	105	31.3	28.7	10.1	107.1	30.3	30.34	11.8	62.0	18.3	12.8
11	10.7	58.2	21.5	11.4	10.3	46.5	19.4	10.27	10.6	32.0	16.5	5.1
12	11.8	88.2	25.6	19.4	11.2	87.2	25.7	21.63	10.4	26.8	14.8	3.9
13	10.1	130	27.2	26.8	10.0	126.6	27.0	26.43	10.8	59.4	22.2	12.1
14	11	132	26.4	22.1	10.0	132.0	26.7	22.75	10.6	38.6	17.0	6.6
15	12.8	61.5	22.0	11.5	12.8	60.0	21.2	11.22	12.2	59.2	19.9	11.2
16	11.7	67.5	33.6	15.2	10.0	67.2	27.5	15.15	10.6	53.0	20.3	10.8
17	10.2	100	26.5	20.1	10.0	100.1	27.4	23.27	10.8	42.4	19.4	8.5
18	12.9	82	24.0	19.9	12.8	88.2	23.5	21.42	13.8	26.2	17.1	3.9
19	10.4	72.3	26.6	15.0	10.2	61.6	27.0	14.54	10.4	64.0	20.7	11.9
21	14.5	42.5	24.5	7.7	14.8	43.4	23.6	7.34	12.8	41.2	19.7	7.0
22	10.8	73.2	23.2	15.4	10.7	71.50	22.3	15.57	14.0	67.4	23.2	12.1
23	10	46	19.9	11.0	10.0	46.8	20.9	11.86	10.4	45.4	18.5	10.1
24	10.8	89.5	24.9	20.4	10.5.	80.0	25.0	19.09	12.0	58.8	19.8	11.3
25	11.9	95	25.9	19.5	11.1	90.7	26.2	21.73	10.6	41.6	17.7	6.8
26	10.3	97.8	23.7	17.4	10.1	95.2	23.8	18.04	10.8	58.0	21.6	11.7
27	10.9	50.9	24.5	12.1	10.8	52.6	22.5	12.01	14.2	35.0	19.9	6.2
28	10	69	25.8	18.1	9.7	71.7	26.9	19.18	12.2	38.0	17.4	6.7
30	10.1	79	27.2	19.4	10.3	76.4	25.3	18.8	11.0	52.6	20.5	11.9
31	10.4	71	21.7	12.3	10.0	61.8	14.1	11.35	12.2	46.6	21.2	7.5
32	10.1	92.9	23.0	17.4	10.1	93.5	22.4	17.91	14	25.2	18.18	3.28
Average	**11.1**	**77.6**	**24.9**	**16.6**	**10.2**	**72.3**	**23.9**	**16.9**	**11.7**	**45.6**	**19.1**	**8.6**

4.4. Tree height measurements

The tree height was measured by three methods. There were (1) manual measurement in field; (2) manual measurement from T-LiDAR data; and (3) automatic extraction from T-LiDAR using in Computree software. Plot level descriptive statistics (minimum, maximum, mean and standard deviation) of tree height measurements by the tree different methods are given in Table 4-4.

From the table, we can see that there are dissimilarities among the plot level tree height measurements statistics (minimum, maximum, mean and standard deviation). The differences between field measured heights and automatically extracted heights are more than the differences between field measured heights and manually measured height from T-LiDAR data. These differences indicate that the height derived by automatic method is less accurate than the height measured by manual measurement from point cloud in compared to field measurements.

Overlapping of tree crowns is the main reason for erroneous estimation of tree height. Due to dense and overlapping crown (Figure 5-6), occlusion occurs (Figure 5-8) which make difficult to target the tree height both in field measurements and manual measurements from T-LiDAR data. Most of the small trees are overestimated due to overlapping with larger trees in automatic height extraction.

Table 4-4. Plot level statistics of tree height measured in field and from T-LiDAR data

Plot	Tree height (m)				T-LiDAR tree height (m)							
	Field measurement				Manual measurement				Automatic measurement			
	Min	**Max**	**Mean**	**Std**	**Min**	**Max**	**Mean**	**Std**	**Min**	**Max**	**Mean**	**Std**
7	10	46	21.4	10.3	7.1	23.7	13.2	4.3	7.0	20.5	16.2	3.5
8	9	40	20.2	8.1	8.3	30.5	18.8	5.6	13.8	28.2	20.4	4.8
9	8	28	17.7	7.9	7.6	26.0	16.4	6.9	8.1	20.2	13.0	7.9
10	4.9	39.4	15.8	7.6	5.2	36.6	17.7	9.3	16.0	31.8	23.3	4.8
11	5.4	38.3	13.5	7.9	5.5	22.3	12.8	4.0	14.5	26.9	22.2	3.4
12	7.6	34.2	13.5	6.2	7.4	27.7	14.1	5.8	7.6	16.8	11.2	7.4
13	5.6	29.3	14.5	7.0	7.3	33.9	15.7	6.8	14.5	32.8	24.9	5.4
14	5.7	35.0	14.2	7.4	8.6	33.7	17.4	5.9	9.1	35.9	24.5	6.7
15	7.6	28.0	15.4	6.1	9.0	25.0	15.8	4.6	13.0	22.9	17.4	2.9
16	10.0	29.1	15.4	5.7	11.0	31.4	18.2	5.8	5.2	31.4	22.2	6.7
17	8.0	36.0	16.5	7.4	10.2	24.9	15.0	3.8	7.8	38.3	20.8	6.1
18	9.5	27.0	14.1	5.4	8.0	27.0	13.8	5.3	8.4	22.8	12.6	4.4
19	5.8	32.0	15.2	6.7	8.5	32.0	17.7	6.2	6.7	37.0	24.8	8.1
21	9.1	24.0	15.0	4.6	9.4	23.7	15.0	4.2	6.7	25.8	19.1	5.4
22	6.5	40.0	15.0	8.0	7.0	23.3	12.9	4.5	9.5	30.1	18.3	5.2
23	8.0	25.2	15.0	4.9	8.1	27.0	15.4	4.9	14.9	27.0	20.1	3.0
24	8.2	23.0	14.2	5.0	9.5	27.7	14.7	5.1	9.7	26.9	16.4	5.9
25	8.4	30.0	15.4	6.1	5.6	26.4	14.1	5.2	9.2	27.5	15.7	4.2
26	8.6	30.0	17.5	7.4	10.7	40.3	17.6	6.7	12.8	35.0	22.1	5.3
27	9.3	26.3	17.4	4.1	12.0	27.9	19.7	5.0	17.2	28.1	22.0	2.8
28	6.5	41.2	17.7	8.9	10.8	40.1	18.9	9.1	11.4	32.8	20.1	5.8
30	5.5	29.5	15.5	7.1	6.2	29.8	14.7	6.8	8.7	26.7	17.2	5.1
31	7.3	25.2	14.5	4.8	5.3	29.6	14.4	5.4	5.4	22.1	16.7	4.4
32	7.7	32.2	14.3	5.0	8.8	29.9	14.3	4.8	12.9	25.4	18.9	3.7
Average	**7.6**	**31.2**	**15.8**	**6.6**	**8.2**	**29.2**	**15.8**	**5.7**	**10.4**	**28.0**	**19.2**	**5.1**

4.5. Comparison of DBH measured from field and manually derived fromT-LiDAR data

Regression analysis was done to compare the relationship between field observation and manually measured DBH from T-LiDAR data. The plot level relationships analyses of the first 12 plots are shown in Figure 4-3 by scattered plots and the rest of the plots are presented in Appendix 2. The summary of fit for DBH comparison is presented in Table 4-5.

The lowest value of R^2 is 0.69 in plot 27 and the highest value is 0.99 in plots 12, 13, 15, 16, 22, 23, 26, 30, and 32. The plots 11, 27, and 31 have outliers which have decreased the overall value of the plot. These outliers are due to occlusion (Figure 5-8) causes from high stem density and undergrowths.

The average value of R^2 for all plots is 0.95, which is reasonably high and very close estimate between the field measurements and T-LiDAR derived DBH. These very close estimate make them very suitable for AGB and AGC estimation with an average RMSE value of 2.7 cm.

Table 4-5. Summary of fit for DBH comparison (field and manual)

Plot	*7*	*8*	*9*	*10*	*11*	*12*	*13*	*14*	*15*	*16*	*17*	*18*
R^2	0.96	0.93	0.98	0.96	0.88	0.99	0.99	0.96	0.99	0.99	0.97	0.97
RMSE	2.3	2.8	1.8	3.5	4.3	1.3	1.5	4.3	1.2	1.4	3.7	3.4
Plot	*19*	*21*	*22*	*23*	*24*	*25*	*26*	*27*	*28*	*30*	*31*	*32*
R^2	0.93	0.96	0.99	0.99	0.96	0.95	0.99	0.69	0.97	0.99	0.91	0.99
RMSE	4.1	1.3	1.4	1.0	2.9	4.6	1.3	6.9	3.3	1.2	4.5	1.5

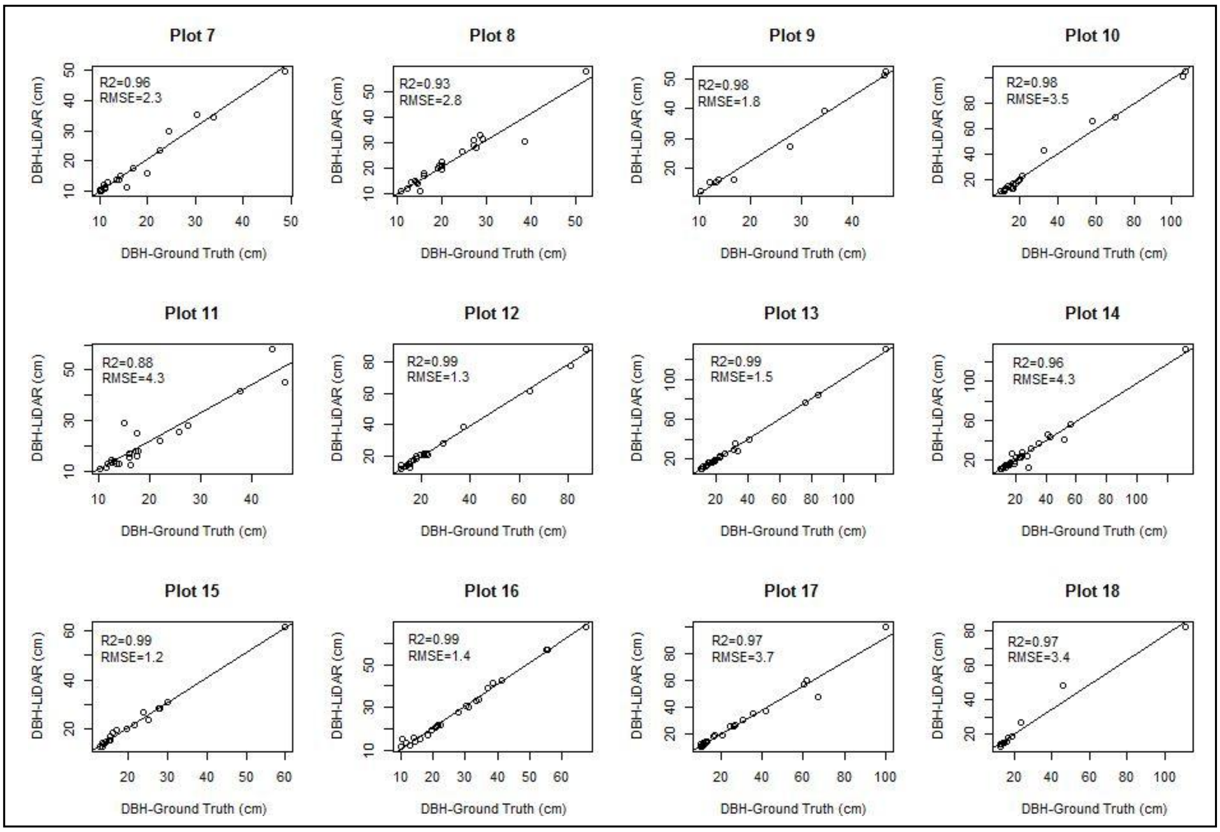

Figure 4-3. Plot level comparison of BDH from field and manually derived from T-LiDAR data

4.6. Comparison of DBH measured from field and atomatically derived from T-LiDAR data

Regression analysis was done to compare the relationship between field observation and automatic derived DBH from T-LiDAR data. The plot level relationships analyses of the first 12 plots are shown in Figure 4-4 by scattered plots and the rest of the plots are shown in Appendix 3. The summary of fit for tree height comparison is presented in Table 4-6.

The lowest value of R^2 is 0.80 for plot 7 and the highest value is 0.99 for plot 23. The scattered plots 7, 11, and 28 have values lower than 0.90 due to outliers which has decreased the overall value of the plot. These outliers are due to occlusion (Figure 5-8) causes from high stem density and undergrowths.

The average value of R^2 of all plots is 0.93, which is very reasonable estimate for the automatic extraction of tree DBH from 3D point cloud data for AGB and AGC estimation with an average RMSE value of 2.29 cm.

Table 4-6. Summary of fit for DBH comparison (field and automatic)

Plot	*7*	*8*	*9*	*10*	*11*	*12*	*13*	*14*	*15*	*16*	*17*	*18*
R^2	0.80	0.92	0.94	0.91	0.88	0.91	0.90	0.93	0.97	0.95	0.96	0.90
RMSE	3.12	2.95	2.5	4.00	2.17	1.30	4.32	2.00	1.9	2.8	1.9	1.2
Plot	*19*	*21*	*22*	*23*	*24*	*25*	*26*	*27*	*28*	*30*	*31*	*32*
R^2	0.93	0.97	0.96	0.99	0.98	0.95	0.97	0.90	0.89	0.91	0.91	0.94
RMSE	3.2	1.0	2.3	0.8	1.3	1.9	1.7	2.3	2.7	3.7	2.7	1.2

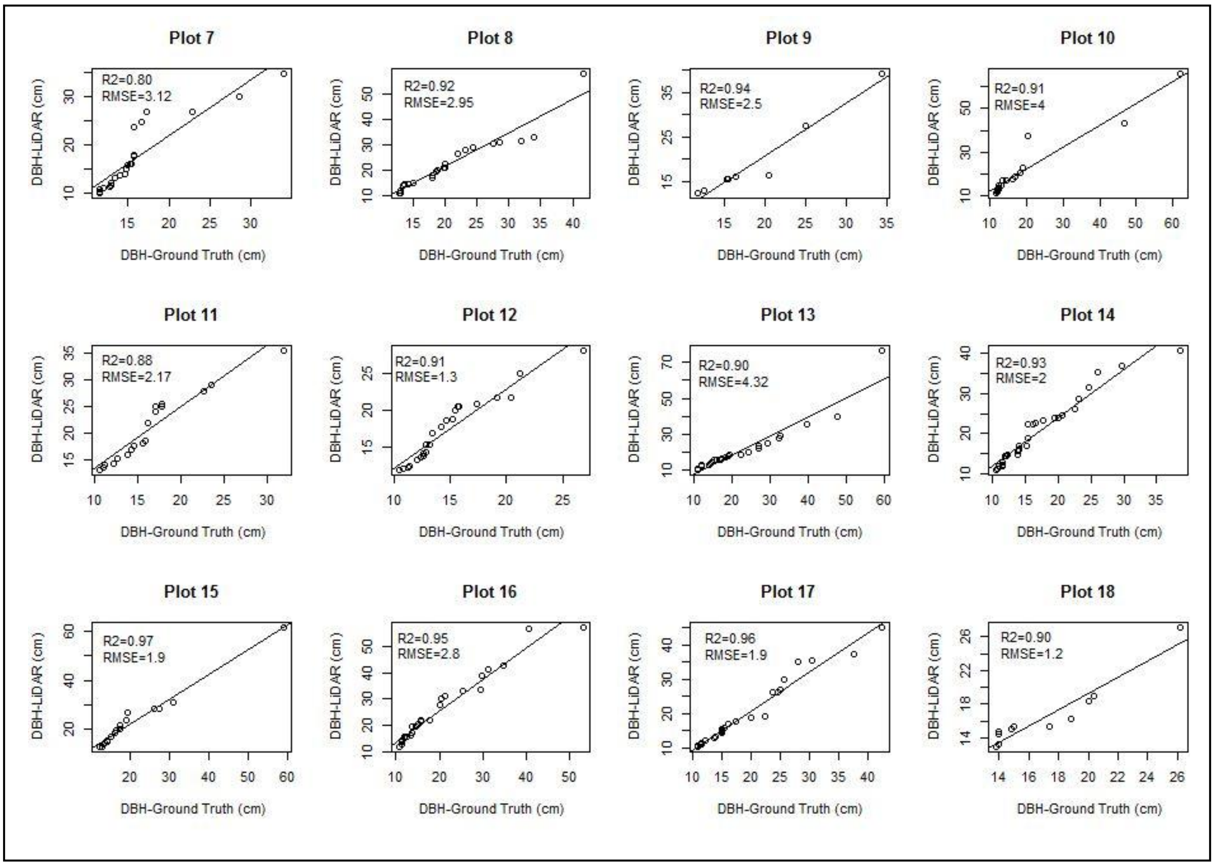

Figure 4-4. Plot level comparison of DBH from field and automatically derived from T-LiDAR data

4.7. Comparison of tree height measured from field and manually measured from T-LiDAR data

Regression analysis was done to compare the relationship between field observations and manually measured tree heights from T-LiDAR data. The plot level relationships analyses of the first 12 plots are shown in Figure 4-5 by scattered plots and the rest of the plots are shown in Appendix 4. The summary of fit for tree height comparison is presented in Table 4-7.

The lowest value of R^2 is 0.38 for plot 11 and the highest values is 0.99 for plot 30. The plots 9, 21, 22, 30 and 32 have R^2 values higher than 0.99, while other plots have lower values due outliers. The main causes of outliers are occlusion (Figure 5-8) and overlapping crown (Figure 5-6) in upper canopy of the trees.

The average value of R^2 of all plots is 0.77, which is a reasonable estimate for the manual extraction of tree height from 3D point cloud data for AGB and AGC estimation with an average RMSE value of 2.96 m.

Table 4-7. Summary of fit for tree height comparison (field and manual)

Plot	*7*	*8*	*9*	*10*	*11*	*12*	*13*	*14*	*15*	*16*	*17*	*18*
R^2	0.82	0.65	0.92	0.78	0.38	0.88	0.79	0.68	0.65	0.87	0.78	0.85
RMSE	4.9	5	2.3	2.8	4.7	2.3	3.2	4.2	3.7	2.0	3.4	2.1
Plot	*19*	*21*	*22*	*23*	*24*	*25*	*26*	*27*	*28*	*30*	*31*	*32*
R^2	0.87	0.96	0.95	0.68	0.61	0.66	0.64	0.53	0.77	0.99	0.7	0.97
RMSE	2.4	0.8	1.6	2.9	3.3	3.7	5.0	2.6	4.9	0.5	2.9	0.8

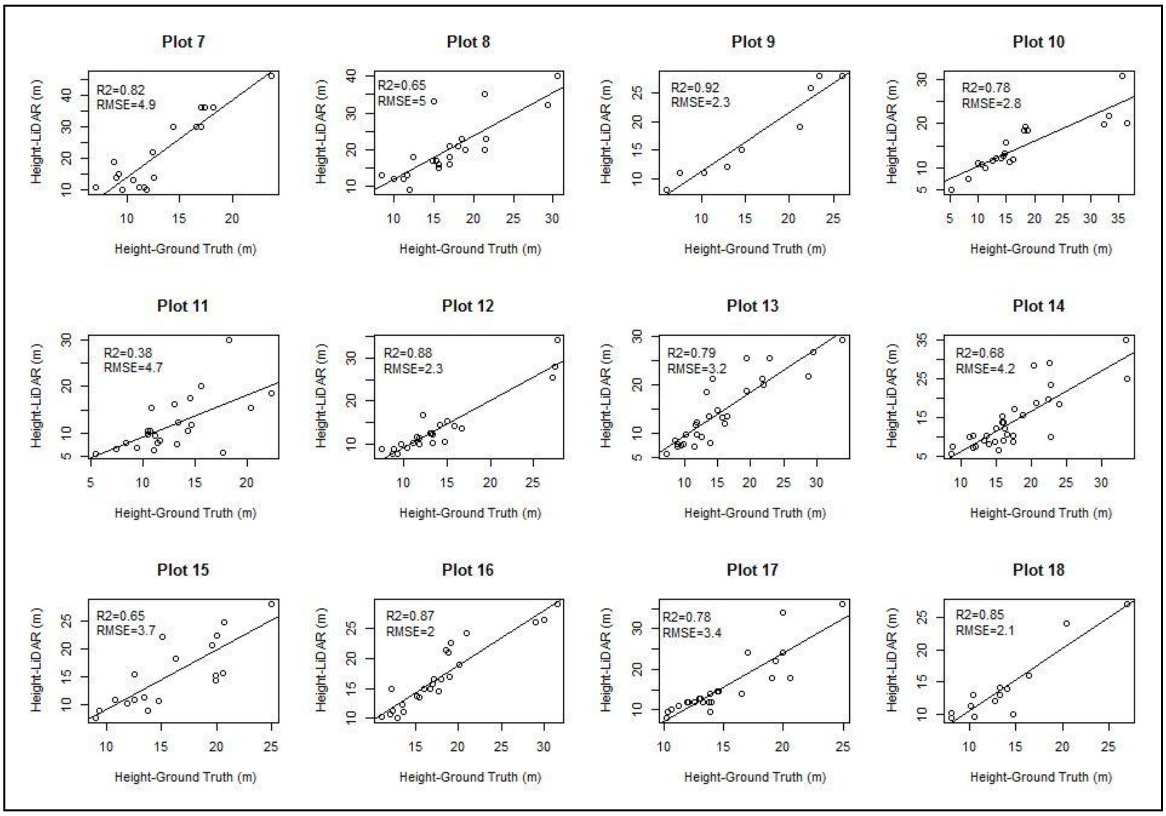

Figure 4-5. Plot level comparison of tree height from field and manually derived from T-LiDAR data

4.8. Comparison of tree height measured in field and automatically derived from T-LiDAR data

Regression analysis was done to compare the relationship between field observation and automatically derived tree height from T-LiDAR data. The plot level relationships analyses of the first 12 plots are shown in Figure 4-6 by scattered plots and the rest of the plots are shown in Appendix 5. The summary of fit for tree height comparison is presented in Table 4-8.

The lowest value of R^2 is 0.0001 for plots 8 and 11, and the highest value is 0.34 for plot 18. In all plots there are many outliers due to occlusion (Figure 5-8) and overlapping crown (Figure 5-6) in upper canopy of the trees. The average value of R^2 of all plots is 0.04, which shows that no reasonable estimate for the automatic extraction of tree height from 3D point cloud data. The average value of RMSE 5.35 m which is also unacceptably large.

The average value of R^2 is 0.04, which indicate that there is no relationships between field measurements of trees height and automatically derived trees heights from T-LiDAR data. Thus, the automatically derived tree heights from T-LiDAR data are not suitable for AGB and AGC estimation.

Table 4-8. Summary of fit for tree height comparison (field and automatic)

Plot	*7*	*8*	*9*	*10*	*11*	*12*	*13*	*14*	*15*	*16*	*17*	*18*
R^2	0.04	0.0001	0.02	0.01	0.0001	0.01	0.08	0.01	0.08	0.09	0.001	0.34
RMSE	8.7	7.3	6.2	4.7	8.0	2.6	6.4	5.6	6.0	5.4	5.4	3.5
Plot	*19*	*21*	*22*	*23*	*24*	*25*	*26*	*27*	*28*	*30*	*31*	*32*
R^2	0.001	0.03	0.01	0.04	0.003	0.01	0.03	0.12	0.08	0.02	0.001	0.002
RMSE	5.8	4.7	7	4.3	5	4.8	5.4	3.1	4.7	6.9	4.7	2.1

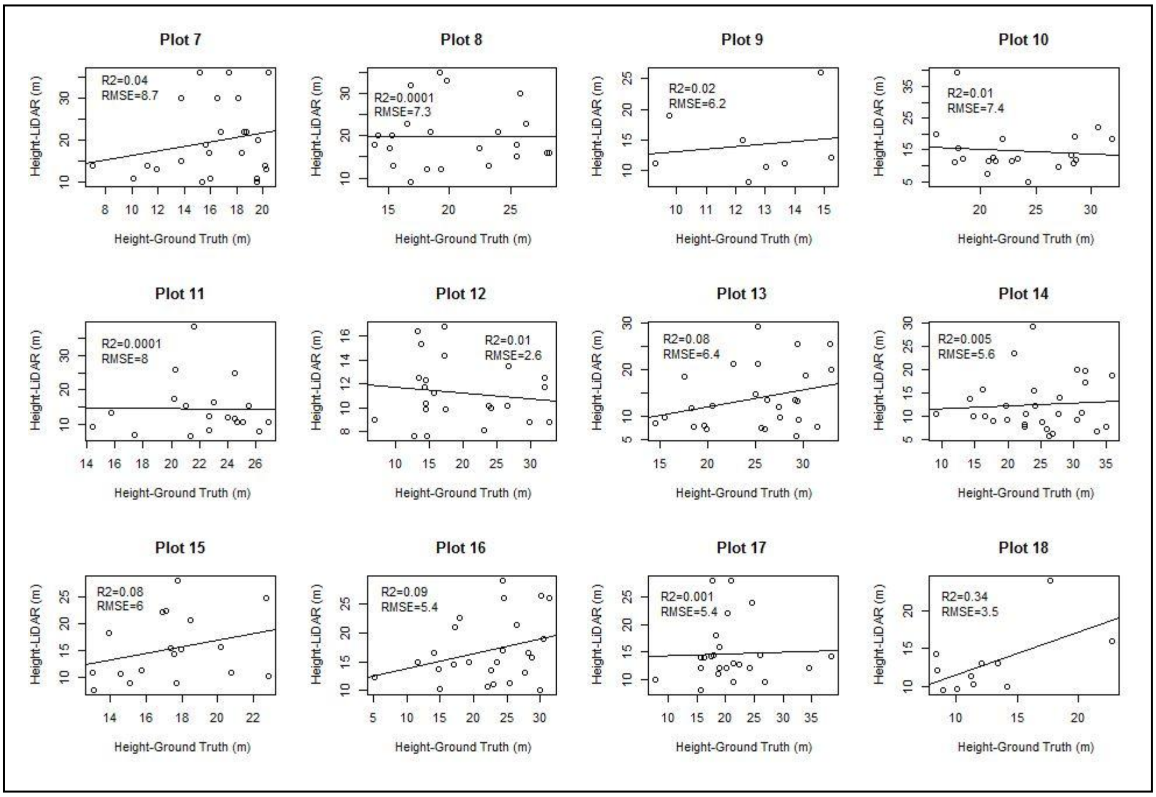

Figure 4-6. Plot level comparison of tree height from field and automatically derived from T-LiDAR data

4.9. T-test analysis

Paired T-test analysis of was done to test research hypotheses set for this study. The hypotheses were tested at 95% critical significant level, i.e., $\propto = 0.05$.

4.9.1. T-test: Paired two sample for means of DBH from field and manually derived from T-LiDAR data

The summary of T-test analysis for field measurement of DBH and manually derived DBH from T-LiDAR data was presented in Table 4-9. The null hypotheses were accepted for plots 7, 8, 10, 11, 12, 13, 14, 17, 18, 19, 22, 23, 24, 25, 26, 27, 28, 31, and 32. This indicates that there is no significant differences between field measured DBH and manually measured DBH from T-LiDAR data for 79% (19 out of 24) of total plots.

Table 4-9 : Summary of T-test statistics for DBH from field and manually derived from T-LiDAR data

Plot	*7*	*8*	*9*	*10*	*11*	*12*	*13*	*14*	*15*	*16*	*17*	*18*
df	17	21	8	19	22	22	27	30	17	24	23	12
t Stat	1.0	1.7	3.9	0.4	1.8	0.4	0.9	-0.2	2.9	2.2	-0.9	-0.5
P(T<=t) two-tail	0.31	0.11	0.00	0.71	0.09	0.72	0.37	0.81	0.01	0.04	0.40	0.60
t Critical two-tail	2.11	2.08	2.31	2.09	2.07	2.07	2.05	2.04	2.11	2.06	2.07	2.18
Plot	*19*	*21*	*22*	*23*	*24*	*25*	*26*	*27*	*28*	*30*	*31*	*32*
df	24	24	24	25	14	20	23	16	18	20	32	21
t Stat	0.8	3.5	1.4	0.6	0.5	0.9	2.0	1.7	-0.7	3.0	0.4	1.8
P(T<=t) two-tail	0.45	0.00	0.17	0.52	0.62	0.37	0.06	0.10	0.46	0.01	0.66	0.09
t Critical two-tail	2.06	2.06	2.06	2.06	2.14	2.09	2.07	2.12	2.10	2.09	2.04	2.08

4.9.2. T-test: Paired two sample for means of DBH from field and automatically derived from T-LiDAR data

The summary of T-test analysis for field measurement of DBH and automatically derived DBH from T-LiDAR data was presented in Table 4-10. The null hypotheses were accepted for plots 7, 9, 13, 17, 18, 26, 19, and 33. This indicates that there is no significant differences between field measurement DBH and automatically derived DBH T-LiDAR data for 33% (8 out of 24) of total plots.

Table 4-10: Summary of T-test statistics for DBH from field and automatically derived from T-LiDAR data

Plot	*7*	*8*	*9*	*10*	*11*	*12*	*13*	*14*	*15*	*16*	*17*	*18*
df	23	21	7	19	18	22	25	28	17	24	24	10
t Stat	1.7	2.2	0.7	2.4	8.4	8.6	-1.4	7.6	4.7	8.2	1.6	-1.6
P(T<=t) two-tail	0.10	0.04	0.50	0.03	0.00	0.00	0.19	0.00	0.00	0.00	0.12	0.13
t Critical two-tail	2.07	2.08	2.36	2.09	2.10	2.07	2.06	2.05	2.11	2.06	2.06	2.23
Plot	*19*	*21*	*22*	*23*	*24*	*25*	*26*	*27*	*28*	*30*	*31*	*32*
df	24	21	24	26	14	23	30	19	17	19	33	18
t Stat	4.3	15.4	-4.2	0.1	2.3	6.5	-0.9	0.3	1.5	2.4	-2.1	-2.3
P(T<=t) two-tail	0.00	0.00	0.00	0.93	0.03	0.00	0.39	0.75	0.15	0.02	0.05	0.03
t Critical two-tail	2.06	2.08	2.06	2.06	2.14	2.07	2.04	2.09	2.11	2.09	2.03	2.10

4.9.3. T-test: Paired two sample for means of tree height from field and manually measured from T-LiDAR data

The summary of T-test analysis for field measurement of tree height and automatically derived tree height from T-LiDAR data was presented in Table 4-11. The null hypotheses were accepted for plots 8, 11, 12, 13, 15, 17, 18, 21, 22, 23, 24, 25, 26, 28, 30, 31, and 32. The null hypothesis were accepted for this indicates that there is no significant differences between field measurement tree height and manually measured tree height from T-LiDAR data for 70% (17 out of 24) of total plots.

Table 4-11: Summary of T-test statistics for tree height from field and manually measured from T-LiDAR data

Plot	*7*	*8*	*9*	*10*	*11*	*12*	*13*	*14*	*15*	*16*	*17*	*18*
df	17	21	8	19	22	22	27	30	17	24	23	12
t Stat	4.7	3.1	2.1	-2.8	-1.1	-0.9	-1.9	-4.3	-0.5	-2.2	0.9	0.7
P(T<=t) two-tail	0.00	0.00	0.07	0.01	0.26	0.39	0.07	0.00	0.60	0.04	0.39	0.51
t Critical two-tail	2.11	2.08	2.31	2.09	2.07	2.07	2.05	2.04	2.11	2.06	2.07	2.18
Plot	*19*	*21*	*22*	*23*	*24*	*25*	*26*	*27*	*28*	*30*	*31*	*32*
df	24	24	24	25	14	20	23	16	18	20	32	21
t Stat	-4.3	-0.1	1.7	-0.3	-0.5	1.8	0.4	-2.4	-0.9	1.5	-0.1	0.6
P(T<=t) two-tail	0.00	0.94	0.09	0.77	0.60	0.09	0.70	0.03	0.40	0.14	0.93	0.55
t Critical two-tail	2.06	2.06	2.06	2.06	2.14	2.09	2.07	2.12	2.10	2.09	2.04	2.08

4.9.4. T-test: Paired two sample for means of tree height from field and automatically derived from T-LiDAR data

The summary of T-test analysis for field measurement of tree height and automatically derived tree height from T-LiDAR data was presented in Table 4-12. The null hypotheses were accepted for plots 7, 8, 9, 15, 18, 24, 25, and 30. This indicates that there is no significant differences between field measurement tree height and automatically derived tree height from T-LiDAR data for 33% (8 out of 24) of total plots.

Table 4-12: Summary of T-test statistics for tree height from field and automatically derived from T-LiDAR data

Plot	*7*	*8*	*9*	*10*	*11*	*12*	*13*	*14*	*15*	*16*	*17*	*18*
df	23	21	7	19	18	22	25	28	17	24	24	10
t Stat	1.94	-0.3	0.7	-4.25	-3.9	-4.9	-7.9	-7.7	-1.4	-3.6	-3.8	0.3
P(T<=t) two-tail	0.06	0.74	0.49	0.00	0.00	0.00	0.00	0.00	0.17	0.00	0.00	0.74
t Critical two-tail	2.07	2.08	2.4	2.093	2.1	2.1	2.1	2.05	2.11	2.1	2.06	2.2
Plot	*19*	*21*	*22*	*23*	*24*	*25*	*26*	*27*	*28*	*30*	*31*	*32*
df	24	21	24	26	14	23	30	19	17	19	33	18
t Stat	-5.5	-3.2	-2.3	-6.48	-1.3	-1.2	-3.6	-4.7	-3.8	-1.4	-2.3	-6.5
P(T<=t) two-tail	0.00	0.00	0.03	0.00	0.20	0.22	0.00	0.00	0.00	0.17	0.03	0.00
t Critical two-tail	2.06	2.08	2.1	2.056	2.14	2.1	2	2.09	2.11	2.1	2.03	2.1

4.10. Above ground biomass and carbon estimation

4.10.1. Above ground biomass and carbon stocks

AGB and AGC of sample plots were estimated using the allometric equation of Chave *et al.,* (2005) from field measured and manually derived T-LiDAR DBH and tree height. The details of AGB and AGC stocks in the sample plots and their extrapolation on per hectare basis are given in Table 4-13. In the plots 10, 13, and 14, the T-LiDAR, AGB and AGC stocks were overestimated while plot 12 is equal to the field, and the rest of the plots were underestimated in comparison with field estimation. The main reason for overestimation is the difference in height measurement. The lowest stock of AGC is 37 Mg ha^{-1} in plot 7 (extrapolated) and the highest is 361 Mg ha^{-1} in plot 10. The average per hectare estimate of biomass and carbon are 286 Mg and 134 Mg on the basis of field observation while 278 Mg and 130 Mg on the basis of T-LiDAR estimation. In comparison of field estimates, AGB and AGC were under estimated by 3%.

Table 4-13. AGB and AGC stocks in the study area

	Field estimation				**T-LiDAR estimation**			
Plot No.	AGB per plot (Mg)	AGC per plot (Mg)	AGB per ha (Mg)	AGC per ha (Mg)	AGB per plot (Mg)	AGC per plot (Mg)	AGB per ha (Mg)	AGC per ha (Mg)
7	8	4	162	76	4	2	79	37
8	10	5	195	92	7	3	144	67
9	6	3	125	59	5	2	91	43
10	28	13	558	262	38	18	769	361
11	7	3	136	64	5	2	102	48
12	18	8	355	167	18	8	356	167
13	30	14	610	286	35	16	700	329
14	35	16	690	324	35	17	706	332
15	7	3	146	68	7	3	133	62
16	14	7	287	135	14	7	282	132
17	21	10	413	194	18	8	353	166
18	7	3	139	65	7	3	146	69
19	14	7	284	133	14	6	273	129
21	7	3	143	67	7	3	133	62
22	13	6	263	124	8	4	163	77
23	9	4	182	85	9	4	180	85
24	10	5	205	96	9	4	181	85
25	15	7	298	140	13	6	259	122
26	22	10	441	207	20	9	395	185
27	7	3	136	64	7	3	135	63
28	17	8	334	157	18	8	357	168
30	14	7	281	132	13	6	264	124
31	10	4	190	89	9	4	190	89
32	15	7	291	137	14	6	272	128
Mean	**14**	**7**	**286**	**134**	**14**	**7**	**278**	**130**

For the sake of visualization of difference in AGB and AGC estimate using field and T-LiDAR measurements, the plot extrapolation of per hectare stock of AGB is plotted in Figure 4-7 and AGC stock is plotted in Figure 4-8. The T-LiDAR heights of trees are overestimated in plots 10, 13, 14 and 28 which have increased the AGB and AGC stocks of these plots.

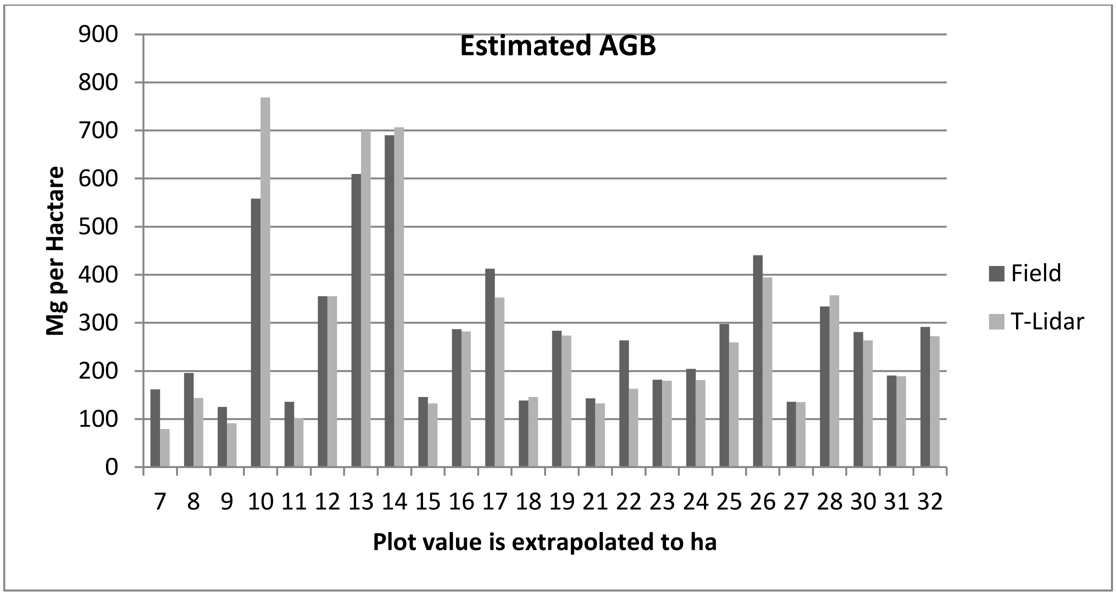

Figure 4-7. Comparison of plot level AGB stocks estimated from field measured and T-LiDAR derived DBH and tree height

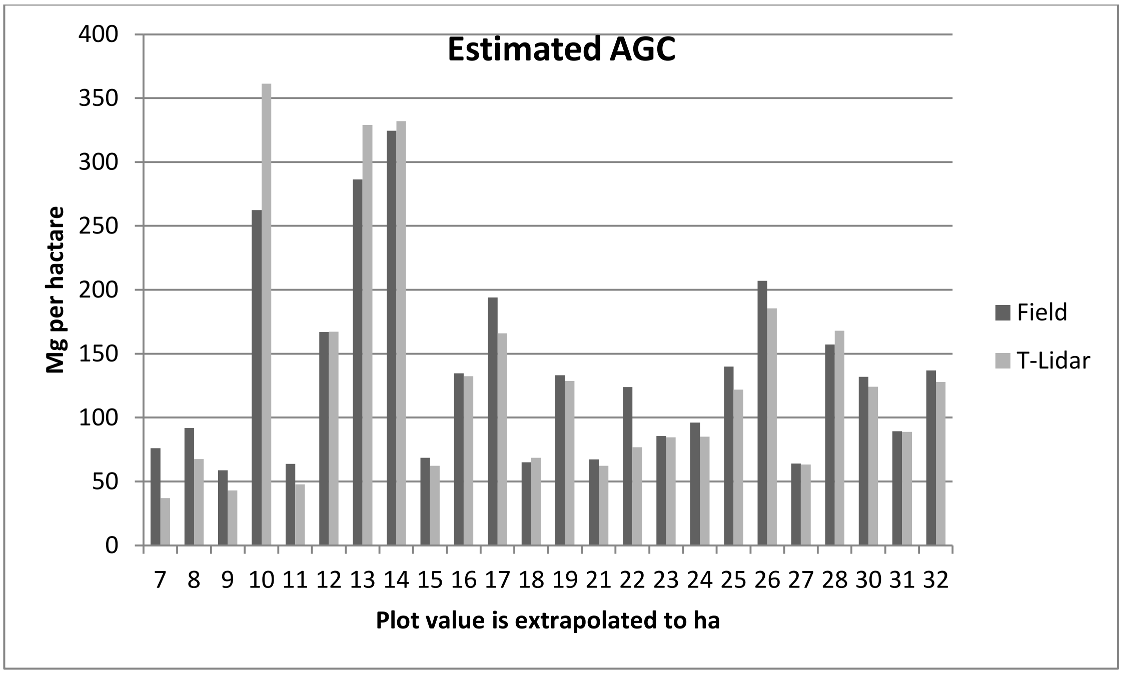

Figure 4-8. Comparison of plot level AGC stock estimated from field measured and T-LiDAR derived DBH and tree height

4.10.2. Comparison between AGB and AGC stocks and accuracy

AGB and AGC were estimated from field measured and manually derived DBH and tree height from T-LiDAR data using the allometric equation. The average per hectare estimate of biomass and carbon are 286 Mg and 134 Mg on the basis of field observation while 278 Mg and 130 Mg on the basis of T-LiDAR estimation (Table 4-9). AGB and AGC derived from field and T-LiDAR were compared with estimated field measurements (Figure 4-9). The R^2 values for both the estimated AGB and AGC is 0.93 and the corresponding RMSE values are 42.4 Mg and 19.9 Mg per hectare. Per hectare RMSE% value for biomass and carbon are 14.8% and 14.8%. These values indicate that AGB and AGC can be estimated with reasonable accuracy using manually derived DBH and tree height from T-LiDAR data compared to field measurement.

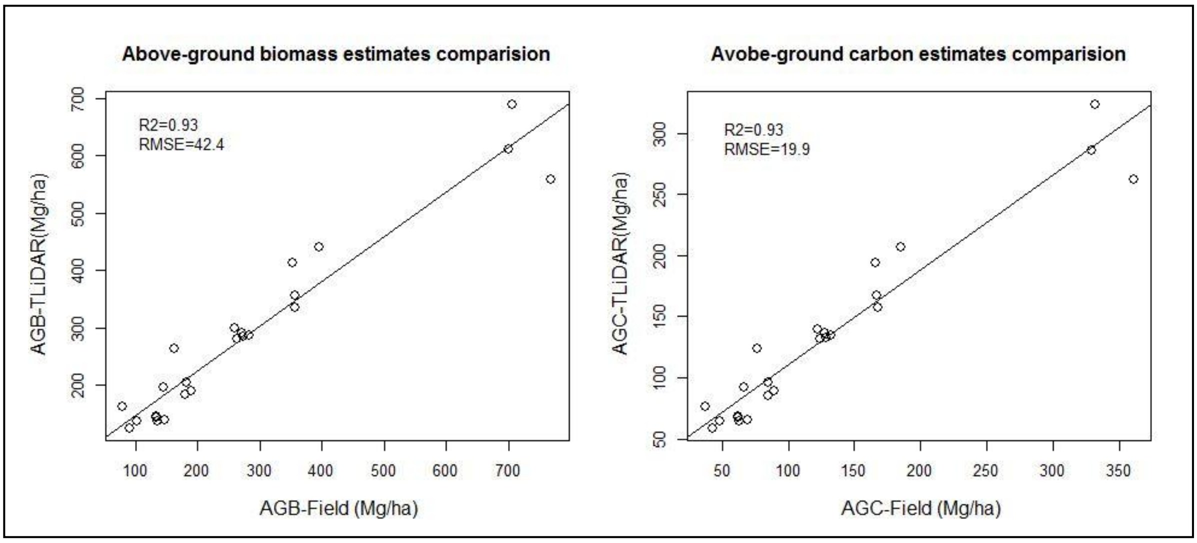

Figure 4-9. Comparison of AGB and AGC stocks, estimated from field measured and T-LiDAR derived DBH and tree height

T-test (Table 4-14) was done to test the significance of AGB and AGB estimated from field measurement and T-LiDAR data and on the basis of this test it was concluded that is not significant difference between AGB and AGC estimated by field measurement and T-LiDAR data.

Table 4-14. T-test: Paired Two Sample for Means of AGB and AGC estimate

	AGB estimate		AGC estimate	
	AGB (Field)	AGB (T-LiDAR)	AGC (Field)	AGC (T-LiDAR)
Mean	286	277.6	134.3	130.4
Variance	24911	38175	5492	8431
Observations	24	24	24	24
Pearson Correlation	0.96		0.96	
df	23		23	
t-stat	0.685		0.673	
P(T<=t) two-tail	0.5		0.508	
t Critical two-tail	2.069		2.069	
Conclusion: Since, t-stat is less than t-critical value and P-value is greater than $\propto = 0.05$, null hypothesis is accepted. This proved that there is not significant different between AGB and AGC estimated by field measurement and T-LiDAR data.				

In the scattered plot (Figure 4-9), the three plots in the top have big diameter trees which make big difference in AGB and AGC stock with respect to other plots. Both the R^2 value and t-test show that AGB and AGC can be accurately estimated with T-LiDAR data in tropical forest. AGB and AGC estimate from T-LiDAR are in very reasonable agreement, because T-LiDAR DBH are very close to the field DBH and the T-LiDAR height and field height are showing reasonable relationship (in case of manual T-LiDAR estimate). If there is an error or high RMSE, it is mostly because of the height estimation is not very accurate. A similar study conducted for biomass estimation by Kankare *et al.,* (2013) in Scots pine and Norway spruce forest, R^2 values were 0.90 and 0.91 and RMSE values were 22.12 kg and 26 kg achieved at tree level.

5. DISCUSSIONS

There is a growing need for accurate and cost-effective methods for mapping and monitoring of tropical forest biomass and carbon. The use of T-LiDAR can provide more accurate reference forest inventory data (Kankare *et al.,* 2013). The main objective of this study was to assess the potentiality of T-LiDAR to derive forest plot inventory parameters to estimate AGB and AGC in tropical forest. The plot inventory parameters (tree location, DBH and tree height) derived from T-LiDAR data were compared with field measurements. AGB and AGC of the sample plots were computed using the allometric equation (Chave *et al.,* 2005) from both field and manually measured DBH and tree height from T-LiDAR data.

5.1. Tree detection and accuracy assessment

To assess the accuracy of tree detection from point cloud data, both manually and automatically detected trees per plot were compared with respect to field observations. The average detection percent by manual method is 89% (Figure 5-1) and by automatic method is 90% (Figure 5-2). In both cases, plots 9, 12, 17, 27, and 29 have lower detection rate, while plots 8, 13, 15, 16, 22, 24, and 31 have higher detection rate compared to mean value. Reason for lower detection in some plots are occlusion (Figure 5-8) caused by dense ground vegetation cover. Some tags were not identified due to occlusion. These results are similar to the results of Othmani *et al.,* (2011). They got an average detection rate of 90.6% with single scan using the Computree algorithm. Although, the automatic detection rate is higher than by manual detection, in many plots the algorithm failed to detect some large diameter trees. This is a drawback of the software.

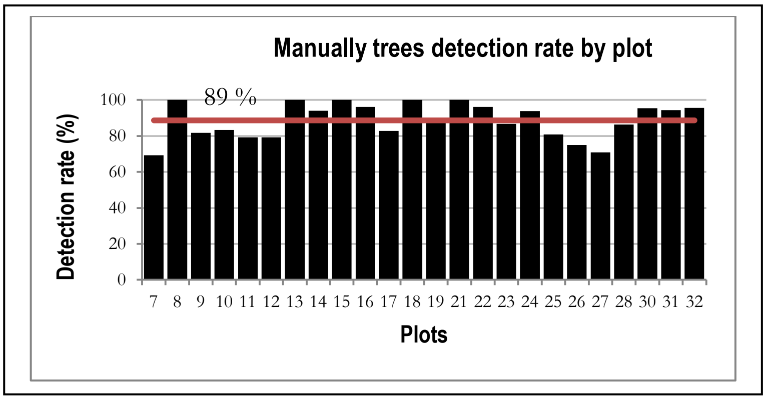

Figure 5-1. Manually trees detection rate by plot

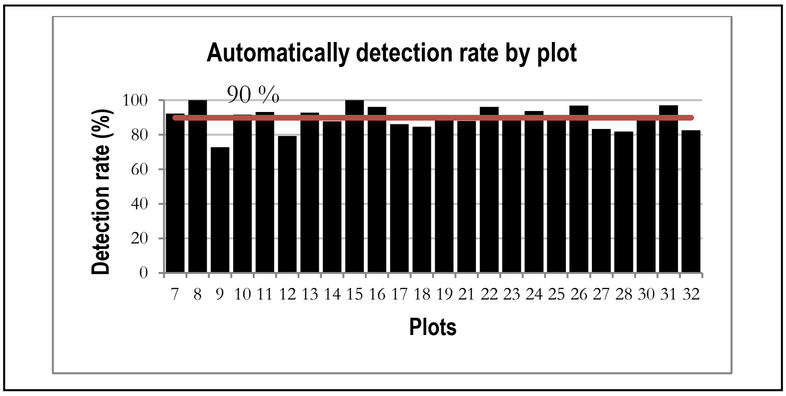

Figure 5-2. Automatically trees detection rate by plot

5.2. DBH estimation and accuracy

In this study, the DBH of tree, one of the most important forest plot inventory parameters, was estimated from T-LiDAR multiple scans point cloud data. It was derived both manually (526 trees) and automatically (530 trees) from the point cloud. The overall comparisons of DBH derived by manual and automatic methods with field measurements are shown in Figure 5-3. The R^2 values for manually and automatically estimated DBH are 0.93 and 0.89 respectively, i.e., 93% and 89% variability in field measured DBH are explained by DBH from T-LiDAR data. The RMSE values are 4.6 cm and 3.3 cm for manual and automatic DBH extractions. These values show that there is high agreements between the DBH derived from T-LiDAR and field measurements.

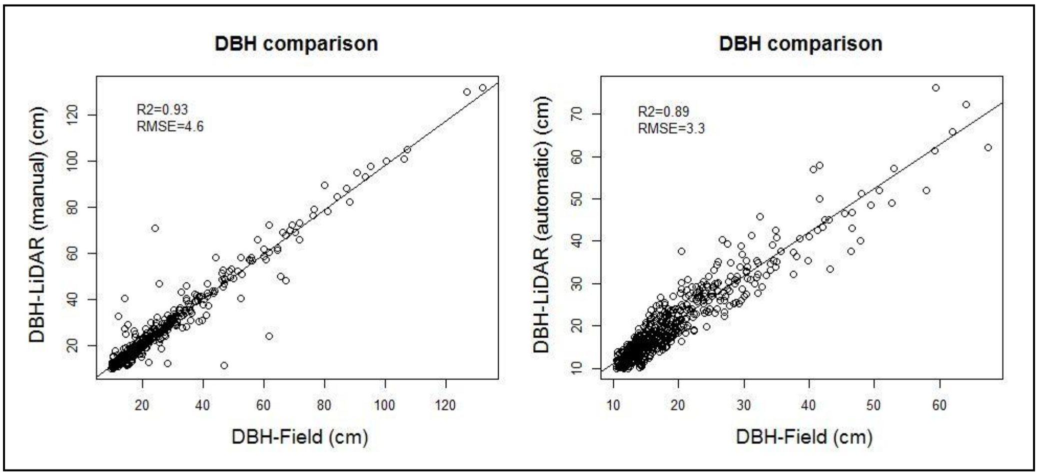

Figure 5-3. Comparison of field measurements with manually and automatically computed DBH from T-LiDAR DATA

Also, the average of plots values of R^2 and RMSE for manual measurement of DBH from T-LiDAR data are 0.95 and 2.7 cm (Table 4-5), which indicates that at plot level 95% of variation in field measurement of DBH is explained by T-LiDAR DBH. Only two plots have R^2 less than 0.90, this due to the occlusion (Figure 5-8) from dense ground vegetation cover present in these plots. The reasons for higher values of R^2 in the maximum number of plots is the low percentage of ground vegetation, which allows good scanning of the trunk of the tree without occlusion. The result of R2 values is also verified by Paired T-test of means for field and manually measured DBH (Table 4-9), which shows that for 79% of plots, there is no difference between field measured DBH and T-LiDAR derived DBH.

Similarly, the average of plots values of R^2 and RMSE for automatic derivation of tree height are 0.93 and 2.29 cm (Table 4-6), which is very reasonable estimate. But in the case of automatic derivation of DBH from T-LiDAR, null hypothesis is accepted only for 33% of plots (Table 4-10). One reason for large variation in results of automatic derivation of DBH was the Computree algorithms did not detect big diameter trees in many plots. The big tree has large stock of biomass, so it alter largely the estimation of biomass and carbon stock. Therefore, automatically derived DBH from T-LiDAR cannot be used for further AGB and estimation. This is the limitation of the software. There is need to develop more a robust algorithm for automatic DBH derivation of the sample plot.

Several studies have similar results which support the findings the this study. Hopkinson *et al.*, (2004) found R^2 value 0.85 for BDH, and regression slope value 1.01 for deciduous forest. In a similar study conducted by Tansey *et al.*, (2009), RMSE values 1.9-3.7 cm was found. In a study conducted by Kankare *et al.,* (2013) in Scots pine and Norway spruce stands, R^2 value 0.95 and RMSE value 1.48 cm were obtained by manual measurement. Similarly, Maas *et al.,* (2008) got RMSE value 1.8 cm in DBH measurement of Spruce and Beech forest inventory plots. According to them there are limitations to use T-LiDAR in natural forest having dense undergrowths in comparison to plantation forest with less complex structure and sparse ground vegetations. Tansey *et al.,* (2009), reported a similar figure for R^2 and RMSE of 3.7 and 1.9 cm computed by cylinder-fitting and circle-fitting. Watt & Donoghue, (2005), found R^2 value 0.92 by circle fitting in conifer plantation forest.

Thus, the values of R^2 and RMSE for DBH estimations by manual methods from T-LiDAR data are consistent with many previous studies conducted in temperate forest, which shows that DBH can be estimated from point cloud data with good accuracy in tropical forest.

5.3. Tree height estimation and accuracy

In this study one of the important forest plot inventory parameter tree height was estimated from T-LiDAR multiple scans point cloud data. The tree height was measured manually and automatically derived from T-LiDAR data. The overall comparison of trees heights derived by manual (526 trees) and automatic (530 trees) method with field measurements are presented in Figure 5-4 (total 526 trees in . The R^2 values for manually and automatically estimated tree heights are 0.62 and 0.002 respectively. The RMSE values are 4.3 m and 5.9 m for manual and automatic tree height estimation. These values show that there is fair agreement between manually derived tree heights from T-LiDAR and field heights measurement, and there is no relationship between automatically derived tree heights derived from T-LiDAR and field tree height measurements.

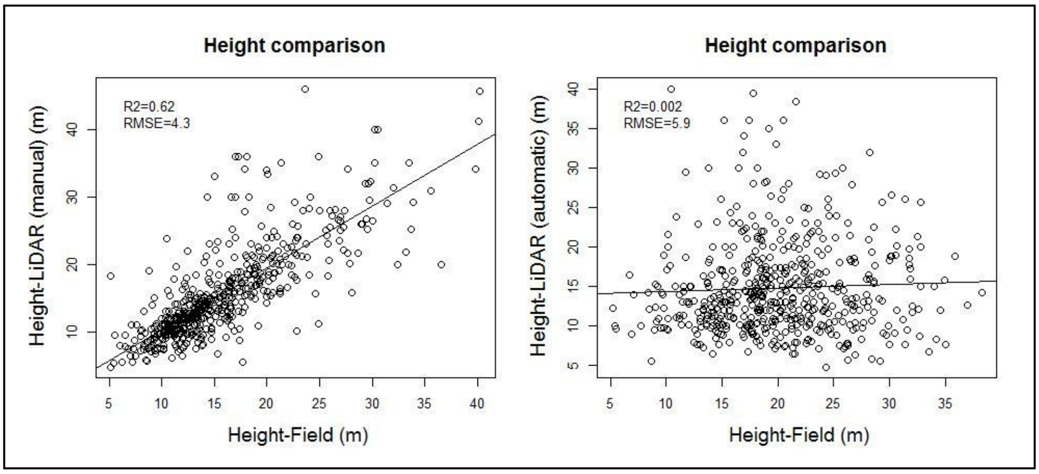

Figure 5-4. Comparison of field measurements with manually and automatically derived tree heights from T-LiDAR data

Also, the average of plots values of R^2 and RMSE for manual measurement of tree height from T-LiDAR data are 0.77 and 2.96 m (Table 4-7), which indicates that at plot level 77% of variation in tree height measurements in field is explained by tree height measurements from T-LiDAR data. Only five plots have R^2 values more than 0.90. The result of R2 values is also verified by Paired T-test of means for field and manually measured tree height (Table 4-11), which shows that for 70% of plots, there is no difference between field measured tree height and T-LiDAR derived tree height.

Similarly, the average of plots values of R^2 and RMSE for automatically derived tree height are 0.04 and 5.35 m (Table 4-8), which is very inaccurate estimate for tree height measurement. The result of T-test also shows that only for 33% of plots there is no difference in field measured tree height and T-LiDAR derived tree height.

The main reason inaccurate estimate tree height is occlusion (Figure 5-8) due to overlapping crown in upper canopy of the trees (Figure 5-6). Due to overlapping crown, in many cases it is impossible to separate whole crown of a tree, particularly for the small tree. In manual extraction of tree from whole plot point cloud data, prior information about crown size is required for more dense crown cover class forest. Thus, manual measurement of tree height from the T-LiDAR data is as subjective as manual tree height measurement in the field.

In this study average manual measurement of tree height was overestimated by approximately 8% in compared to the field measurement (Table 4-4). But In a study by Hopkinson *et al.*, (2004), they found R^2 value 0.86, and regression slope 1.08 for deciduous forest. In their study, the tree height was underestimated by 7% in comparison to mean of field measured height. According to them intervening foliage obstructing the view which leads to leads to systematic under estimation of tree height derived by T-LiDAR. Thus, this study contradicts with the finding of Hopkinson *et al.,* (2004), and shows that tree height can be measured more accurately in comparison to field measurement. In the field as shown in Figure 5-6, due to the big crown size of tree B, it is difficult to locate the actual peak of the tree. This phenomenon leads to underestimation of large tree. The reason for the improvement in the height measurement is may be due to the improvement in capacity of T-LiDAR or may be human error. Therefore, further research is necessary to test the accuracy of tree height measurement using T-LiDAR data.

In the case of automatic estimation of tree heights, the plots wise values of R^2 are very unrealistic (Table 4-8 and Figure 4-8). The average value of R^2 for all plot is 0.04, which shows that the tree height derived from T-LiDAR data does not explain variability in tree height in the field. This shows that it is not possible to derive tree height from CHM in the case of T-LiDAR data. In this study, the corresponding Z value associated with tree stem was computed using CHM, but the heights of many small trees have been over estimated. From the Figure 5-4, it is apparent that the agreement among field observed heights and T-LiDAR heights are weakest for the tallest trees. Due to crown overlapping with big trees, the small trees were overestimated. As shown in Figure 5-5, CHM over estimates the height of trees A and C. Although, CHM is very popular and successful method for derivation of tree height from airborne LiDAR data, this method is not suitable for T-LiDAR data.

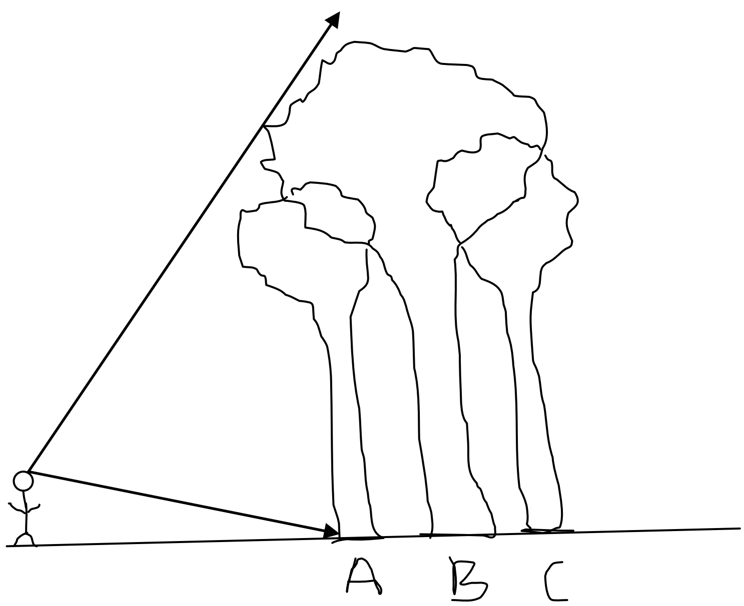

Figure 5-5. Error in height measurement due to crown overlapping

In a similar study carried out into Martinshaw Wood, located at the nearby of Leicester (UK) by Tansey *et al.,* (2009), they found that automatic measurement of tree height in plots with high stand density (1000 stems per hectare) is not possible. Similarly, Maas *et al.*, (2008) found RMSE of 4.5m, which is also unacceptably large. Therefore, it is necessary to develop a robust method for automatic tree height extraction from T-LiDAR point cloud data.

The R^2 values for manual measurement of tree height of plot 11 and 30 are 0.38 and 0.99 are also verified by the hemispherical photographs from the plots (Figure 5-6 and Figure 5-7). The photograph of plot 11 has more dense and overlapping crown compared to the photograph of plot 30.

Figure 5-6. Hemispherical photograph from plot 11, showing dense and overlapping canopy

Figure 5-7. Hemispherical photograph from plot 30, showing relatively open canopy

5.4. Comparison of manual and automatic T-LiDAR data processing

T-LiDAR technology has the capacity to enhance measurement of forest inventory parameters in tropical forest. For this study the T-LiDAR point cloud was processed both manually and automatically. Both methods have their advantages and disadvantages for extraction of forest inventory parameters and AGB and AGC estimation.

The software available for manual processing are 3D Reshaper, CloudCompare, PointStream, MeshLab, and RiSCAN PRO. These generic software packages are suitable for visualization and manipulation of point clouds. According to Chapman *et al.* (2010), these generic data processing software have some user friendly tools like selection, shape fitting but these software are not necessarily adapted to forest environments which compels to look for other solutions. For this study manual extraction of individual tree was carried out in RiSCAN PRO software. After that, measurement of DBH and tree height were done in both RiSCAN PRO and CloudCompare software.

The software available for automatic processing T-LiDAR data for the forestry applications are very limited. The automatic processing software available are Computree, SimpleTree, and AutoStem$_{TM}$. For this study, automatic processing was carried in Computree software. This is an open source software managed by the French National Forestry Office. While automatic estimation of DBH shows promising results with R^2 value is 0.93, the tree detection was less accurate. Tree height was extracted in ArcGis 10.2.2 from CHM generated in Computree. The R^2 value for automatic tree height extinction is 0.04, which is very low. However, this study found some consistency in the error. In most of the sample plots the Computree algorithms failed to detect some large diameter trees.

Although manual measurement of tree height from T-LiDAR data has shown promising results with R^2 value 0.77, the automatic method failed to reliably estimate tree height. One of the main reasons for this is the overlapping of tree crowns due to the dense forest crown cover. In most of the cases the height of small trees is overestimated due to overlapping with neighbouring large trees.

This study shows that the T-LiDAR data can be useful for derivation of the forest inventory parameters for AGB and AGC estimations. Manual measurements have given satisfactory result for tree detection, and DBH and tree height estimation from T-LiDAR data. In case of automatic data processing, this study shows that tree detection and DBH can be measured with some satisfactory results. This study suggests that the performance of an algorithm might vary from one forest type to another, or from temperate to tropical forest. As a result, the Computree software is not suitable for inventory parameters in tropical forest.

The results of manual measurements show that T-LiDAR data has potential for derivation of forest plot inventory parameters. However, manual processing is subjective, tedious and time-consuming job. For forestry applications, automatic processing methods of T-LiDAR data appear to be more applicable but more robust automatic algorithms are required to derive forest plot inventory parameter in tropical forest. Until now, most of the software have been developed and tested in conifer forests. Although Computree software is very useful platform for automated extraction, some improvement is necessary for detection of big diameter tree. This study also revealed that there is necessary to develop algorithms for tropical forest.

5.5. Sources of errors

The accuracy of forest inventory parameter measurement depend on several factors. One of the main factors is occlusion, which is caused by the intermediate objects between the sensor (source) and target object. The shadow causes by occlusion are main the sources of errors in DBH and tree height measurement both in field (specially tree height) and T-LiDAR measurement. The other sources of error in DBH and tree height measurements are human errors. The error in the automatic derivation of inventory parameters depend upon the quality of scan and the algorithm used. According to Côté *et al.*, (2011), the quality of point cloud obtained from T-LiDAR depends upon the amount of object occlusion and external factors, such as wind, rain, fog, and relative humidity.

In the field measurement of DBH, it is not always possible to measure DBH exactly at 1.3 m above the ground. Some trees have buttresses at the base and so DBH should be measured at end point of deformities. In tropical forest some trees are very large and it is then not possible to measure DBH at finishing point of deformities. Measurement of DBH is highly affected by the shape of stem of tree. Similarly, loose rounding of DBH measuring tape also contributes to over measurement of DBH.

Plot 24_Tree no. 8 Plot 24_Tree no 2

Figure 5-8. Examples of occlusions: In tree no. 8, the half of the portion of the tree bole (black part) has very low point cloud density. In tree no. 2, crown branches is not properly scanned.

Manual DBH measurement from T-LiDAR data are affected by stem form(Kankare *et al.*, 2013). This variation is due to noncircular shape of the trunk. The reading of two perpendicular diameters are not equal. In this study one diameter reading at 1.3 was measured. In T-LiDAR data some trees have shadows due to occlusion at base of the trunk as shown in Figure 5-8 (tree no. 8), DBH was measured below and above the shadow and average was taken.

Similarly, error in height measurement in the field and from the automatic height extraction is described in section 5.3. In manual measurement from T-LiDAR data, error occurs due to occlusion. In the Figure 5-8 (Tree no. 2), the crown is not fully scanned. If the whole crown is not scanned, it leads to underestimation of tree height.

The allometric equation is another major source of error which contribute in accumulated error in biomass estimation along with the error from DBH, tree height, wood density.

5.6. Application for REDD+ MRV

REDD+ program has been implementing in many tropical forest to cope with impact of climate change. Accurate estimates of carbon stock enhancements are crucial for assessing the mitigation benefits for REDD+ projects (Angelsen *et al.*, 2012). This study was done to assess the potentiality T-LiDAR to estimate AGB and AGC in tropical forest.

DBH, tree height, crown diameter, and specific density are major parameters for estimation of AGB and AGC stocks using allometric equations. Among them DBH and tree height are most important forest inventory parameters. Tree height is also used for model development and verification for estimation of biomass and carbon in large area using airborne LiDAR.

This study shows that manual measurement of DBH from T-LiDAR data can be achieved with reasonable accuracy in comparison to traditional field measurement. In the case of tree height measurement, however, there is large variability up to 3 m between field measurement and T-LiDAR measurement. The biomass and carbon estimated from the manually measured DBH and tree height using allometric equation shows that T-LiDAR has can estimation 14.8% of actual stocks in tropical forest. However, manual processing of T-LiDAR data is time consuming task and is also just as subjective as traditional field measurements.

In the case of automatic derivation of plot inventory parameters, DBH was extracted with reasonable accuracy, but the Computree algorithm used for automatic detection of tree was failed to detect some large diameters tree in the plot. Also tree height computation from CHM was not satisfactory.

Thus, this study shows T-LiDAR technology has potential for accurate estimation of biomass and carbon estimation in tropical forest. For application of T-LiDAR technology as an operational tool to facilitate REDD+ programme, automatic processing methods is more suitable in compared to manual method. Nevertheless, there is a need for development of robust algorithms for automatic derivation of plot inventory parameters in tropical forest.

5.7. Limitation of the study

- Available software for manual processing of T-LiDAR data is not user friendly for forestry applications.
- Fully-fledged automatic extraction of plot inventory parameters was not explored due to limited software availability.
- In tropical forest limited research has been done about application of T-LiDAR.

6. CONCLUSIONS AND RECOMMENDATIONS

6.1. Conclusions

In this study, forest plot inventory parameters (DBH and tree height) were collected from field observations and T-LiDAR data of the plot were collected through multiple scanning. DBH and tree height of sample trees were measured manually and computed automatically from the T-LiDAR data.

AGB and AGC were estimated from both field and manually derived DBH and tree height from T-LiDAR data using allometric equation, and parameters were compared to answer the research questions formulated to meet the objectives of this study.

How accurately are trees detected from multiple-scans of T-LiDAR data?

Plot wise average manual and automatic detection rate of trees were 89% and 90% respectively with respect to field observations. In both cases, around 10% trees were not detected.

Can forest inventory parameters (DHB and tree height) be derived manually and automatically from T-LiDAR point cloud data?

In the case manually measured DBH and tree height from T-LiDAR data, paired T-test results confirmed that there were no differences between means of DBH and tree height for 79% and 70% of plots, measured manually from field and T-LiDAR data respectively. Thus, the results of T-test suggest that the forest inventory parameters can be derived manually from T-LiDAR data.

In the case of automatically derived DBH and tree height from T-LiDAR data, paired T-test results confirmed that there were differences between means of DBH and tree height for 67% and 67% of plots, measured manually from field and derived automatically form T-LiDAR data respectively. Thus, the results of T-test suggest that the forest inventory parameters cannot be derived automatically from T-LiDAR data using Computree algorithms.

How accurately can forest inventory parameters (DBH and tree height) be derived from the T-LiDAR data?

The average of plot values of R^2 and RMSE for manual and automatic derivation of DBH were 0.95, 2.7 cm and 0.93, 2.29 cm respectively, i.e., in plot, DBH of tree can be measured with 2.7 cm and 2.29 cm accuracy from T-LiDAR data respectively.

Similarly, the average of plot values of R^2 and RMSE for manual measurement and automatic derivation of tree height were 0.77, 2.96 m and 0.04 and 5.35 m respectively, i.e., in plot, tree height can be measured with 2.96 m and 5.35 m accuracy from T-LiDAR data respectively.

How much AGB and AGC are stored in per hectare forest of the study area?

The AGB and AGC stocks estimated from field measured DBH and tree height were between 136-690 Mg ha^{-1} and 64-324 Mg ha^{-1} respectively. Similarly, the AGB and AGC stocks estimated from manually measured DBH and tree height from T-LiDAR data were between 79-706 Mg ha^{-1} and 37-361 Mg ha^{-1} respectively.

The average stocks of AGB and AGC estimated from field measured DBH and tree height were 286 Mg ha^{-1} and 134 Mg ha^{-1} respectively. Similarly, the average stocks of AGB and AGC estimated from manually measured DBH and tree height from T-LiDAR data were 278 Mg ha^{-1} and 130 Mg ha^{-1} respectively.

How accurately AGB and AGC can be estimated from T-LiDAR data?

The R^2 values for both the estimated AGB and AGC were 0.93 and corresponding RMSE values are 42.4 Mg ha^{-1} and 19.9 Mg ha^{-1} respectively. Similarly, RMSE% values for AGB and AGC were 14.8% , i.e., AGB and AGC can be estimated with 14.8% accuracy by manually measured DBH and tree height from T-LiDAR data in compare to field measured DBH and tree height.

Thus, this study shows that T-LiDAR technology has potential to derive forest plot inventory parameters (stem detection, BDH, and tree height) for AGB and AGC estimation in tropical forest. Comparing with field measurement, these parameters was manually measured with reasonable accuracy from T-LiDAR data. However, manual processing is subjective, tedious and time-consuming job. Automatic derivation of these parameters was not very successful. There is a need to develop robust algorithms for automatic derivation of forest inventory parameters.

6.2. Recommendations

This study shows that T-LiDAR point cloud data has potentiality to improve tropical forest plot inventory parameters measurements. In comparison to traditional manual field inventory method, T-LiDAR data can be acquired rapidly and is less susceptible to subjective judgement. However, still some more studies are necessary for understanding of full applicability of T-LiDAR for AGB and AGC estimation for REDD+. On the basis of this research, the following topics have been recommended for further studies.

- The results of automatic extraction of DBH using Computree algorithms was very encouraging, but there is still possibility to develop more robust algorithms, which can improve accuracy in biomass and carbon estimation in tropical forest.

- Although the results of manual measurements of tree heights are satisfactory, automatic computation of tree height by computing Z value from CHM was unsuccessful. So, there is an opportunity to develop a more robust algorithm for tree height estimation from T-LiDAR data.

- Multiple scans of the sample plot require more time in scanning and data processing, which also take more space for data storage. Therefore, there is a need to develop algorithms for computation forest inventory parameters from single scan.

- AGB and AGC estimation using general allometric equations have error due to variability among species and sites. There is an opportunity develop an algorithm for direct computation of volume from T-LiDAR point cloud data, which can reduce errors due to allometric equation.

LIST OF REFERENCES

Andersen, H., & McGaughey, R. (2004). A comparison of forest canopy models derived from LIDAR and INSAR data in a Pacific Northwest conifer forest. *International Archives of Photogrammetry and Remote Sensing*, (34), 211–217.

Angelsen, A., Brockhaus, M., Sunderlin, W., & Verchot, L. (2012). *Analysing REDD+: Challenges and choices* (pp. 247–260). Indonesia: Center for International Forestry Research. Retrieved from http://books.google.com/books?hl=en&lr=&id=UXx99aBLvFEC&oi=fnd&pg=PR3&dq=Analysing+REDD+%2B+Challenges+and+choices&ots=zUMl4wkZWw&sig=A-p31ckUjouhkzd0ZTTk0jqrOb4

Bienert, A., Scheller, S., Keane, E., Mullooly, G., & Mohan, F. (2006). Application of Terrestrial Laser Scanners for the detrmination of Forest Inventory Parameters. *International Archives of Photogrammetry, Remote Sensing and Spatial Information Sciences*, (36).

Brown, S. (2002). Measuring carbon in forests: current status and future challenges. *Environmental Pollution*, *116*(3), 363–372. doi:10.1016/S0269-7491(01)00212-3

Calders, K., Newnham, G., Burt, A., Murphy, S., Raumonen, P., Herold, M., … Kaasalainen, M. (2014). Nondestructive estimates of above-ground biomass using terrestrial laser scanning. *Methods in Ecology and Evolution*, n/a–n/a. doi:10.1111/2041-210X.12301

Castedo, F., Gómez, E., Diéguez, U., Barrio, M., & Crecente, F. (2012). Aboveground stand-level biomass estimation: a comparison of two methods for major forest species in northwest Spain. *Annals of Forest Science*, *69*(6), 735–746. doi:10.1007/s13595-012-0191-6

Chapman, J., Hung, I., & Tippen, J. (2010). Evaluating TIFFS (tool box for LiDAR data filtering and forest studies) in deriving forest measurements from LiDAR data, *2*(2), 145–152.

Chave, J., Andalo, C., Brown, S., Cairns, M. a, Chambers, J. Q., Eamus, D., … Yamakura, T. (2005). Tree allometry and improved estimation of carbon stocks and balance in tropical forests. *Oecologia*, *145*(1), 87–99. doi:10.1007/s00442-005-0100-x

Clark, M., Roberts, D., Ewel, J., & Clark, D. (2011). Estimation of tropical rain forest aboveground biomass with small-footprint lidar and hyperspectral sensors. *Remote Sensing of Environment*, *115*(11), 2931–2942. doi:10.1016/j.rse.2010.08.029

Computree. (2013). *Jean-Philippe Lang*. Retrieved October 15, 2014, from http://rdinnovation.onf.fr/projects/computree/wiki/Fr_wiki

Côté, J.-F., Fournier, R. a., & Egli, R. (2011). An architectural model of trees to estimate forest structural attributes using terrestrial LiDAR. *Environmental Modelling & Software*, *26*(6), 761–777. doi:10.1016/j.envsoft.2010.12.008

Dassot, M., Constant, T., & Fournier, M. (2011). The use of terrestrial LiDAR technology in forest science: application fields, benefits and challenges. *Annals of Forest Science*, *68*(5), 959–974. doi:10.1007/s13595-011-0102-2

Drake, J. B., Dubayah, R. O., Knox, R. G., Clark, D. B., & Blair, J. B. (2002). Sensitivity of large-footprint lidar to canopy structure and biomass in a neotropical rainforest. *Remote Sensing of Environment*, *81*(2-3), 378–392. doi:10.1016/S0034-4257(02)00013-5

Eysn, L., Pfeifer, N., Ressl, C., Hollaus, M., Grafl, A., & Morsdorf, F. (2013). A Practical Approach for Extracting Tree Models in Forest Environments Based on Equirectangular Projections of Terrestrial Laser Scans. *Remote Sensing*, *5*(11), 5424–5448. doi:10.3390/rs5115424

FAO. (2010). Global Forest Resources Assessment 2010: Main Report. Retrieved July 08, 2014, from http://www.fao.org/forestry/fra/fra2010/en/

Feliciano, E. a., Wdowinski, S., & Potts, M. D. (2014). Assessing Mangrove Above-Ground Biomass and Structure using Terrestrial Laser Scanning: A Case Study in the Everglades National Park. *Wetlands*. doi:10.1007/s13157-014-0558-6

Gábor, B. (2013). *Locating and parameter retrieval of individual trees from terrestrial laser scanner data*. PhD Thesis. The University of West Hungary (Sporon).

Geosystems, L. (2015). HDS Laser Scanners & SW - Leica Geosystems. Retrieved October 10, 2014, from http://www.leica-geosystems.com/en/HDS-Laser-Scanners-SW_5570.htm

Holopainen, M., Vastaranta, M., & Hyyppä, J. (2014). Outlook for the Next Generation's Precision Forestry in Finland. *Forests*, *5*(7), 1682–1694. doi:10.3390/f5071682

Hoover, C. M. (Ed.). (2008). *Field Measurements for Forest Carbon Monitoring*. USA: Springer. doi:10.1007/978-1-4020-85062-2

Hopkinson Chris, Laura Chasmer, Young-Pow Colin, and T. P. (2004). Assessing forest metrics with a ground-based scanning lidar. *Canadian Journal of Forest Research*, *583*, 573–583. doi:10.1139/X03-225

IPCC. (2006). 2006 IPCC Guidelines for National Greenhouse Gas Inventories Volume 4 Agriculture, Forestry, and Other Land Use. Retrieved August 24, 2014, from http://www.ipcc-nggip.iges.or.jp/public/2006gl/vol4.html

Kankare, V., Holopainen, M., Vastaranta, M., Puttonen, E., Yu, X., Hyyppä, J., … Alho, P. (2013). Individual tree biomass estimation using terrestrial laser scanning. *ISPRS Journal of Photogrammetry and Remote Sensing*, *75*, 64–75. doi:10.1016/j.isprsjprs.2012.10.003

Lefsky, M. A., Cohen, W. B., Parker, G. G., & Harding, D. J. (2002). Lidar Remote Sensing for Ecosystem Studies. *Bioscience*, *52*(1), 19–30. Retrieved from http://bioscience.oxfordjournals.org

Liang, X., Litkey, P., Hyyppa, J., Kaartinen, H., Vastaranta, M., & Holopainen, M. (2012). Automatic Stem Mapping Using Single-Scan Terrestrial Laser Scanning. *IEEE Transactions on Geoscience and Remote Sensing*, *50*(2), 661–670. doi:10.1109/TGRS.2011.2161613

Maas, H. G., Bienert, A., Scheller, S., & Keane, E. (2008). Automatic forest inventory parameter determination from terrestrial laser scanner data. *International Journal of Remote Sensing*, *29*(5), 1579–1593. doi:10.1080/01431160701736406

Montaghi, A., Corona, P., Dalponte, M., Gianelle, D., Chirici, G., & Olsson, H. (2013). Airborne laser scanning of forest resources: An overview of research in Italy as a commentary case study. *International Journal of Applied Earth Observation and Geoinformation*, *23*, 288–300. doi:10.1016/j.jag.2012.10.002

Næsset, E. (2011). Estimating above-ground biomass in young forests with airborne laser scanning. *International Journal of Remote Sensing*, *32*(2), 473–501. doi:10.1080/01431160903474970

Ni-Meister, W., Lee, S., Strahler, A. H., Woodcock, C. E., Schaaf, C., Yao, T., & Blair, J. B. (2010). Assessing general relationships between aboveground biomass and vegetation structure parameters for improved carbon estimate from lidar remote sensing. *Journal of Geophysical Research*, *115*, G00E11. doi:10.1029/2009JG000936

Othmani, A., Piboule, A., Krebs, M., Stolz, C., & Voon, L. F. C. L. Y. (2011). Towards automated and operational forest inventories with T-Lidar. *Hobart*, *SilviLaser*(Oct. 16-19), 1–9.

Riegl Laser Management Systems. (2015a). RIEGL - Gallery. Retrieved October 11, 2014, from http://www.riegl.com/nc/products/terrestrial-scanning/gallery/

Riegl Laser Management Systems. (2015b). Terrestrial laser scanning. Retrieved October 15, 2014, from http://www.riegl.com/nc/products/terrestrial-scanning/

Ruiz, L., Hermosilla, T., Mauro, F., & Godino, M. (2014). Analysis of the Influence of Plot Size and LiDAR Density on Forest Structure Attribute Estimates. *Forests*, *5*(5), 936–951. doi:10.3390/f5050936

S.Suksuwan. (2006). Royal Belum State Park. *WWF-Malaysia*. Retrieved July 29, 2014, from http://www.wwf.org.my/about_wwf/what_we_do/forests_main/forest_protect/protect_projects/project_royal_belum/

Tansey, K., Selmes, N., Anstee, a., Tate, N. J., & Denniss, a. (2009). Estimating tree and stand variables in a Corsican Pine woodland from terrestrial laser scanner data. *International Journal of Remote Sensing*, *30*(19), 5195–5209. doi:10.1080/01431160902882587

Trochta, J., Král, K., Janik, D., & Adam, D. (2013). Arrangement of terrestrial laser scanner positions for area-wide stem mapping of natural forests. *Canadian Journal of Forest Research*, *363*(February), 355–363. Retrieved from http://www.nrcresearchpress.com/doi/abs/10.1139/cjfr-2012-0347

UNFCCC. (1997). *Kyoto Protocol to the United Nations Framework Convention on Climate Change.* (pp. 1–60). Retrieved from http://unfccc.int/kyoto_protocol/items/2830.php

UNFCCC. (2011). Essential Background - Durban outcomes. *UNFCC*. Retrieved August 22, 2014, from http://unfccc.int/key_steps/durban_outcomes/items/6825.php

UNFCCC. (2012). Kyoto Protocol. Retrieved June 01, 2014, from http://unfccc.int/kyoto_protocol/items/2830.php

UN-REDD. (2008). UN-REDD Programme. Retrieved June 01, 2014, from http://www.un-redd.org/aboutredd/tabid/102614/default.aspx

USAID. (2013). *REDD+ Measurement, Reporting and Verification (MRV) Manual* (pp. 1–160). Washington, DC. Retrieved from http://pfbc-cbfp.org/news_en/items/redd-measurement-USAID-EN.html

Vonderach, C., Vögtle, T., Adler, P., & Norra, S. (2012). Terrestrial laser scanning for estimating urban tree volume and carbon content. *International Journal of Remote Sensing*, *33*(21), 6652–6667. doi:10.1080/01431161.2012.692888

Watt, P. J., & Donoghue, D. N. M. (2005). Measuring forest structure with terrestrial laser scanning. *International Journal of Remote Sensing*, *26*(7), 1437–1446. doi:10.1080/01431160512331337961

Zanne, A. E., Lopez-Gonzalez, G., Coomes, D. A., Ilic, J., Jansen, S., Lewis, S. L., … Chave, J. (2015). Data from: Towards a worldwide wood economics spectrum. *Dryad.* doi:10.5061/dryad.234

APPENDICES

Appendix 1: The list of local and scientific name of plants found in the study area and their specific density

S.N.	Local Name	Scientific Name	Density	S.N.	Local Name	Scientific Name	Density
1	Temponek	*A. hispidus*	0.58	30	Meranti Sekawang air	*Meranti Sekawang air*	0.58
2	Pulai	*Alstonia spp.*	0.37	31	Merawang Kelabu	*Merawang Kelabu*	0.58
3	Mersawa	*Anisoptera*	0.54	32	Penarahan	*Myristicaceae.*	0.49
4	Mempisang	*Annonaceae.*	0.49	33	Rambutan	*Nephelium lappaceum*	0.73
5	Karas (gaharu)	*Aquilaria malaccensis*	0.32	34	Nytoh	*Palaquium spp.*	0.55
6	Keladang	*Artocarpus*	0.32	35	Pelung	*Pentaspadon motleyi*	0.5
7	Keledang	*Artocarpus spp.*	0.58	36	Perah	*Pimelodendron spp.*	0.46
8	Terap	*Artocarpus spp.*	0.58	37	Melembu	*Pterocambium javanicum*	0.4
9	Belimbing	*Averrhoa bilimbi*	0.47	38	Ludai	*Sapium spp.*	0.4
10	Diam Rambai	*Baccaurea motleyana*	0.51	40	Kulim	*Scorodocarpus Borneensis*	0.76
11	Bintagor	*Calophyllum spp.*	0.53	41	Balau Hitam	*Shorea atrinervosa*	0.75
12	Berangan	*Castanopsis spp*	0.51	42	Meranti	*Shorea leprosula*	0.43
13	Geronggang	*Cratoxylum arborescens*	0.4	43	Meranti Paya	*Shorea platycarpa*	0.58
14	Keranji	*Dialium spp.*	0.8	44	Melantai	*Shorea spp.*	0.61
15	Keruing Pipit	*Dipterocarpus fagineus Vesque*	0.78	45	Meranti Buaya	*Shorea spp.*	0.61
16	Keruing	*Dipterocarpus spp.*	0.61	46	Meranti Mangkai	*Shorea spp.*	0.61
17	Sesenduk	*Endospermum malaccense*	0.46	47	Meranti Sarang Punai	*Shorea spp.*	0.61
18	Tembusu	*Fagraea fragrans*	0.68	48	Meranti Tembaga	*Shorea spp.*	0.61
19	Hopea auriculata Foxw	*Hopea auriculata Foxw*	0.74	49	Sepetir	*Sindora spp.*	0.54
20	Merawan Ungu	*Hopea bracteata Burck*	0.55	50	Akasia	*syn. Acacia greggii*	0.58
21	Giam	*Hopea spp.*	0.64	51	Kelat Jambu	*Syzygium spp.*	0.69
22	Merbau	*Intsia (Afzelia) palembanica*	0.68	52	Seputih	*Trypanosoma sp.*	0.58
23	Kempas	*Koompassia Malaccensis*	0.72	53	Resak Paya	*Vatica lobata Foxw*	0.58
24	Menpening	*Lithocarpus sp.*	0.71	54	Resak	*Vatica spp.*	0.69
25	Pagar Anak	*Lxonanthes spp.*	0.58	55	Kelong		0.58
26	Balik Angin	*Mallothus biaceae*	0.58	56	Kemian		0.58
27	Machang	*Mangifera spp.*	0.52	57	Kubing		0.58
28	Bedang	*Mastixia trichotoma Blume*	0.39	58	Simpul Gajah		0.58
29	Meranti sekawan merah	*Meranti sekawan merah*	0.58	59	Teke		0.58

Appendix 2: Plot level comparison of DBH from field and manually measured from T-LiDAR data (continuation of Figure 4-3)

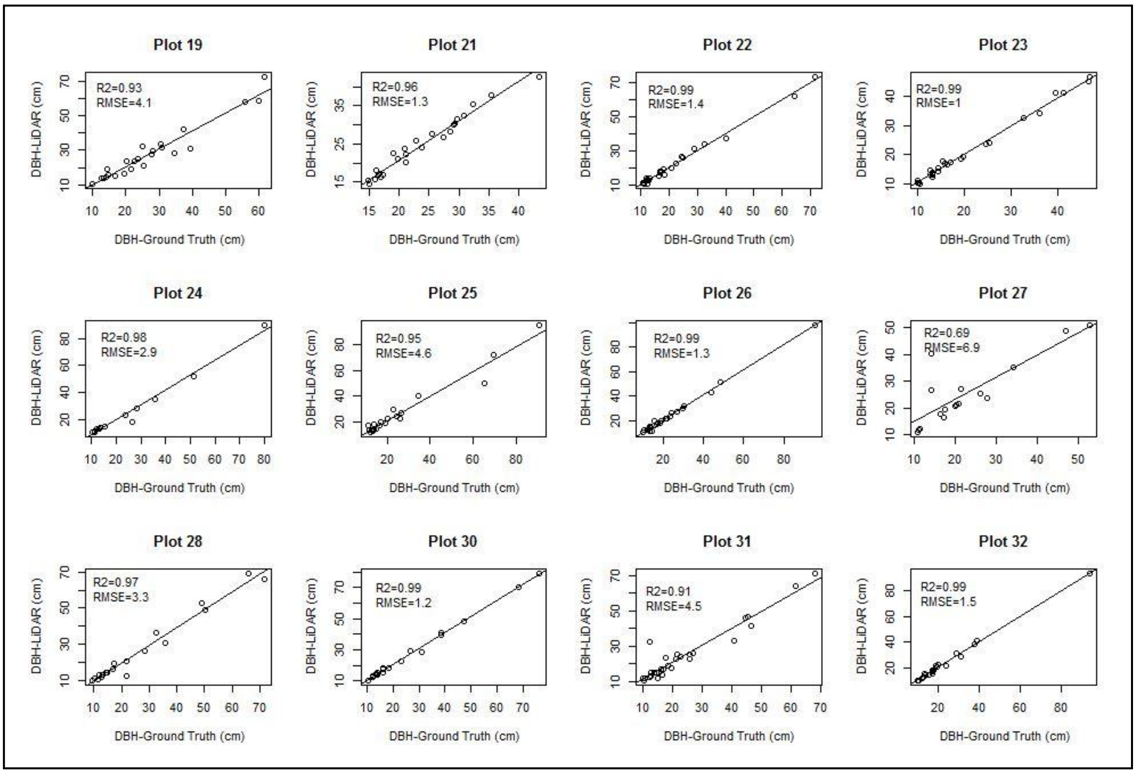

Appendix 3: Plot level comparison of DBH from field and automatically derived from T-LiDAR data (continuation of Figure 4-4)

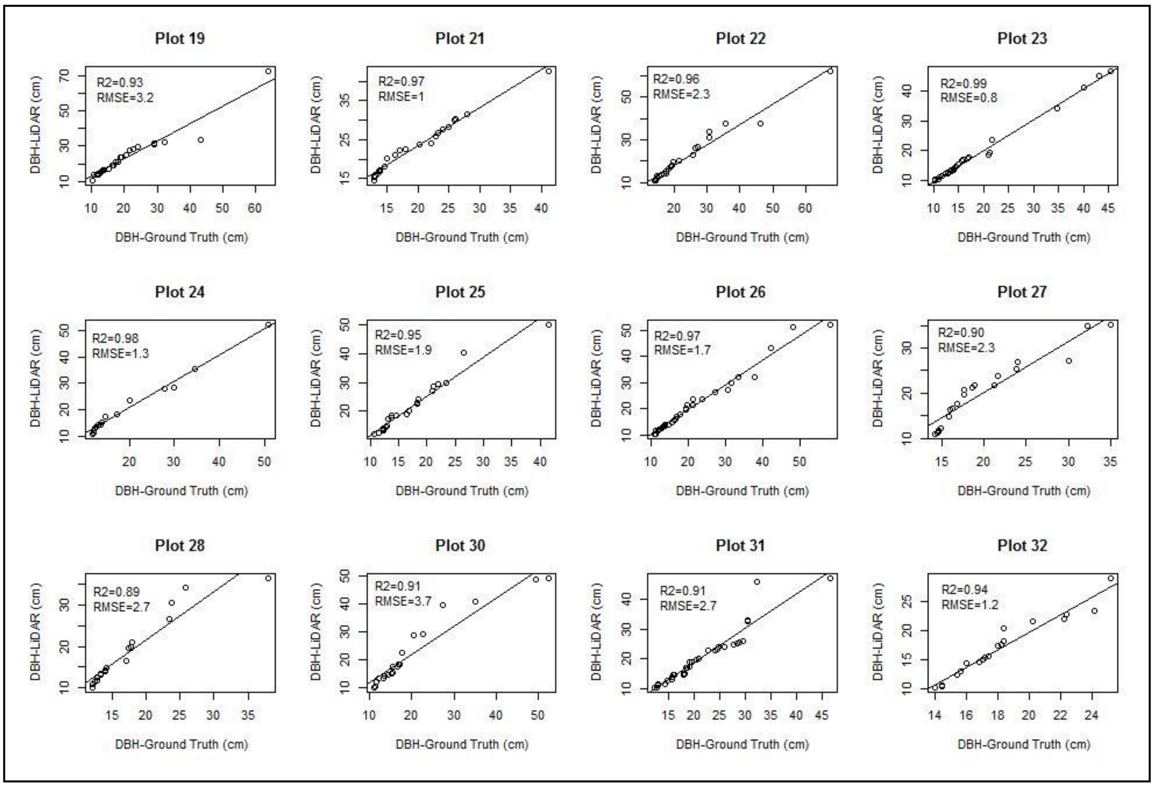

Appendix 4: Plot level comparison of tree heights from field and manually measured from T-LiDAR data (continuation of Figure the 4-5)

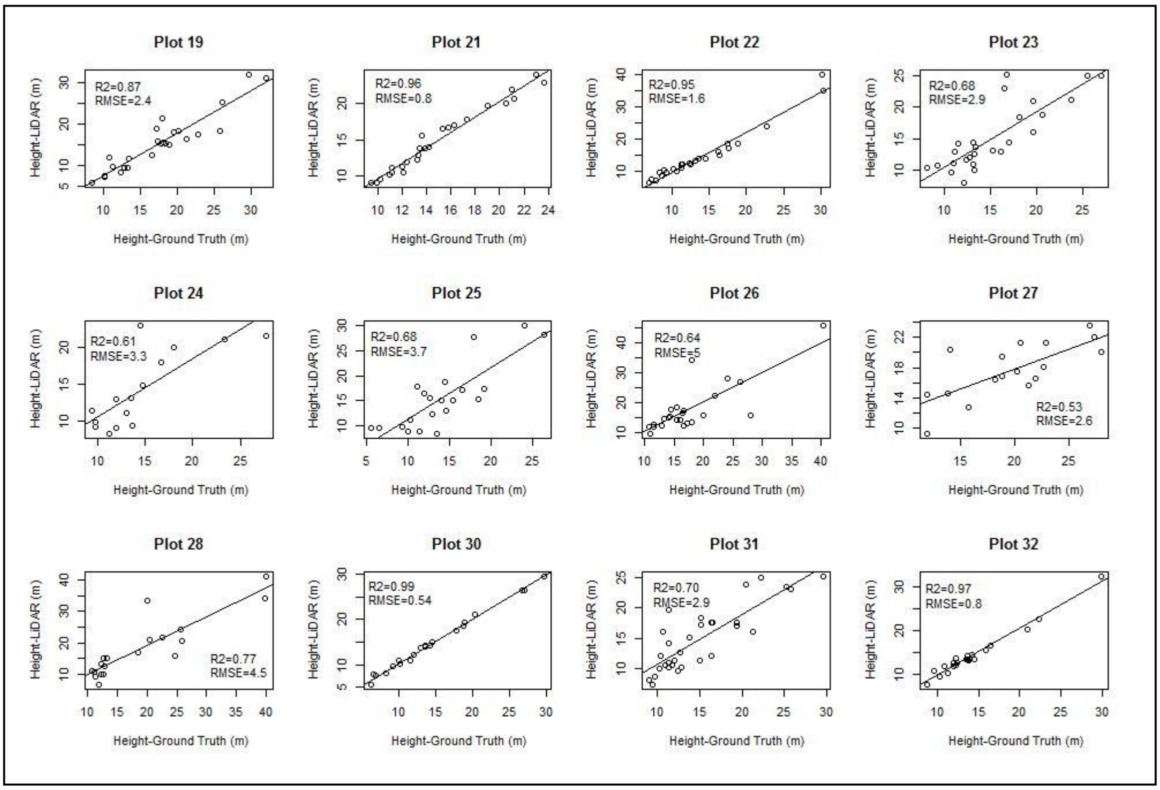

Appendix 5: Plot level comparison of tree height from field and automatically derived from T-LiDAR data (continuation of Figure the 4-6)

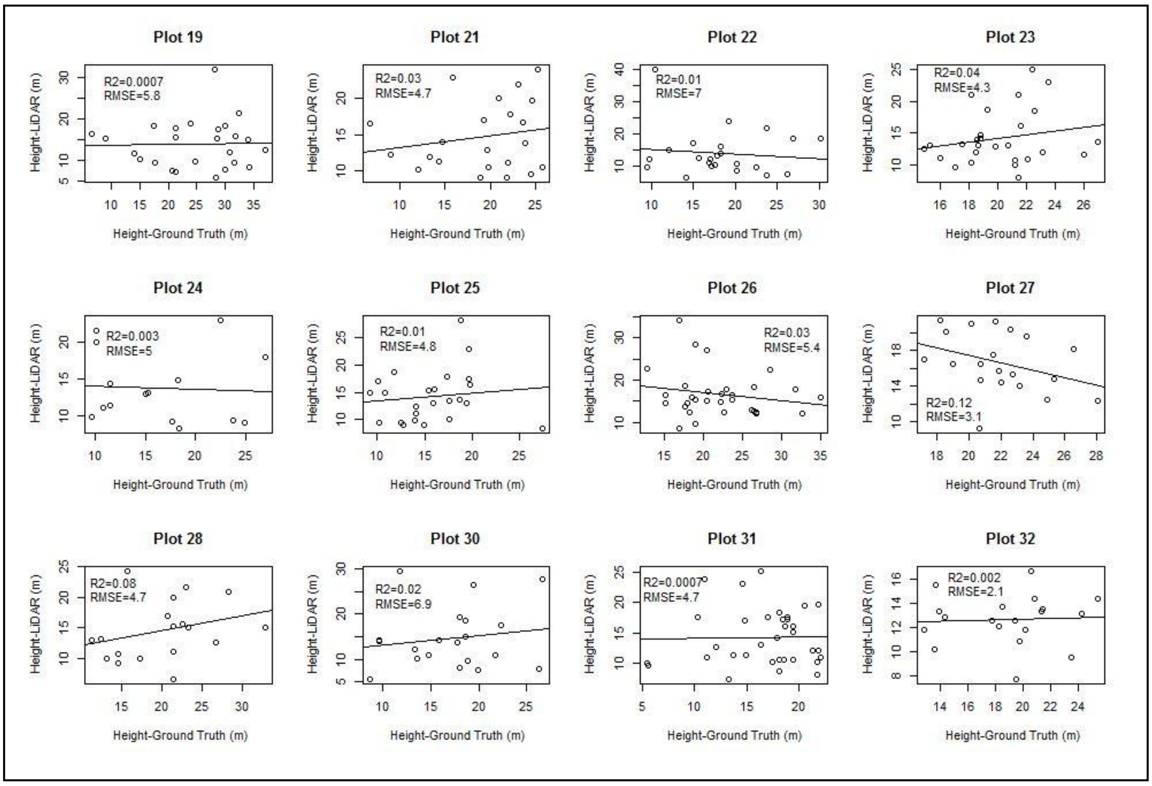

Appendix 6: Steps for automatic extraction of DBH in Computree software

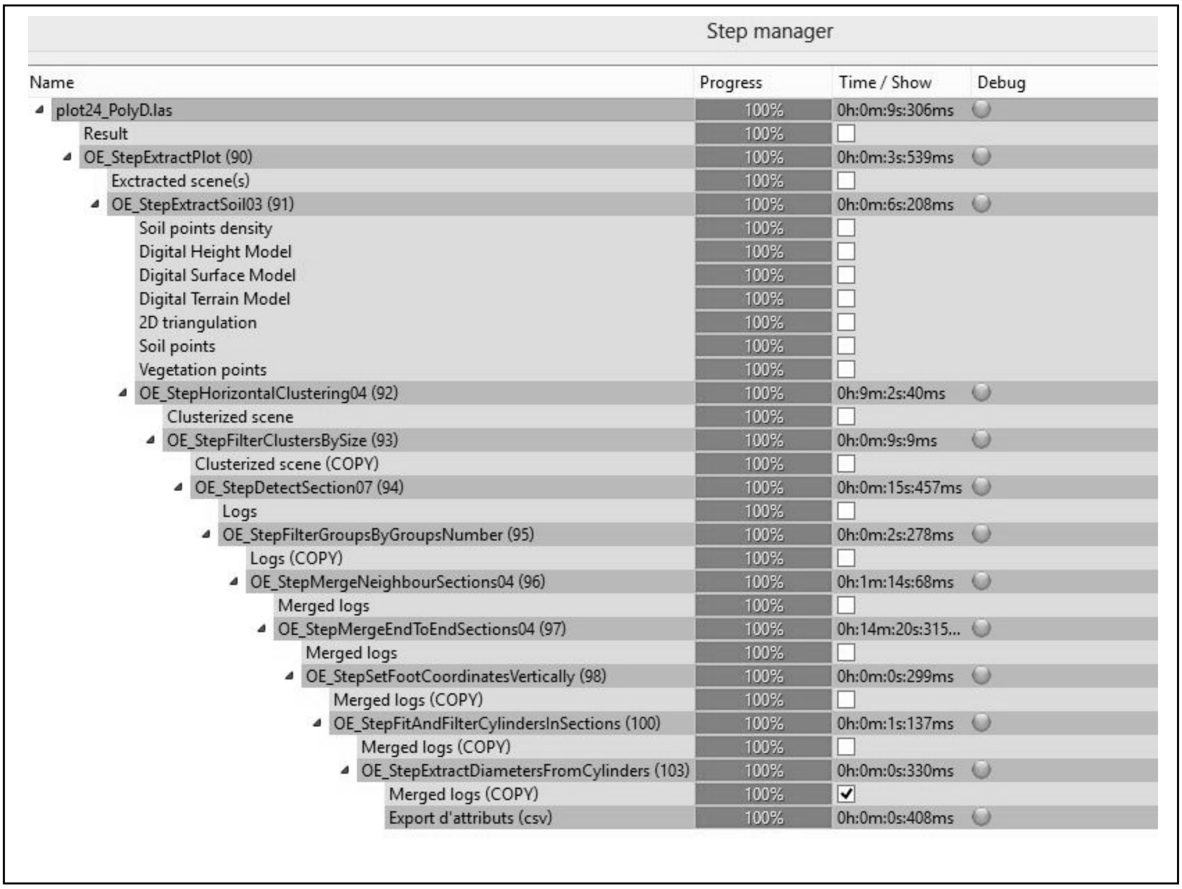

Step manager

Name	Progress	Time / Show	Debug
plot24_PolyD.las	100%	0h:0m:9s:306ms	
Result	100%		
OE_StepExtractPlot (90)	100%	0h:0m:3s:539ms	
Exctracted scene(s)	100%		
OE_StepExtractSoil03 (91)	100%	0h:0m:6s:208ms	
Soil points density	100%		
Digital Height Model	100%		
Digital Surface Model	100%		
Digital Terrain Model	100%		
2D triangulation	100%		
Soil points	100%		
Vegetation points	100%		
OE_StepHorizontalClustering04 (92)	100%	0h:9m:2s:40ms	
Clusterized scene	100%		
OE_StepFilterClustersBySize (93)	100%	0h:0m:9s:9ms	
Clusterized scene (COPY)	100%		
OE_StepDetectSection07 (94)	100%	0h:0m:15s:457ms	
Logs	100%		
OE_StepFilterGroupsByGroupsNumber (95)	100%	0h:0m:2s:278ms	
Logs (COPY)	100%		
OE_StepMergeNeighbourSections04 (96)	100%	0h:1m:14s:68ms	
Merged logs	100%		
OE_StepMergeEndToEndSections04 (97)	100%	0h:14m:20s:315...	
Merged logs	100%		
OE_StepSetFootCoordinatesVertically (98)	100%	0h:0m:0s:299ms	
Merged logs (COPY)	100%		
OE_StepFitAndFilterCylindersInSections (100)	100%	0h:0m:1s:137ms	
Merged logs (COPY)	100%		
OE_StepExtractDiametersFromCylinders (103)	100%	0h:0m:0s:330ms	
Merged logs (COPY)	100%	✓	
Export d'attributs (csv)	100%	0h:0m:0s:408ms	

Appendix 7: Sample plot inventory sheet

Sample plot inventory sheet

Plot No.:	Date:	Recorder's:
Slope (%):	Canopy density: 1. 2. 3. 4.	Average:
FCD Class No.:	Undergrowth:	

Scan Position	X- Coordinate	Y-Coordinate	Z-Coordinate	Remarks
Central position				
Outer scan position-1				
Outer scan position-2				
Outer scan position-3				
Remarks (Circular reflector) - 1				
Remark -2				
Remark -3				

S.N.	X-Coord	Y-coord	Z-coord	DBH (cm)	Height (m)	Crown Diam (m)	Species	Remarks

Appendix 8: Some photographs from field